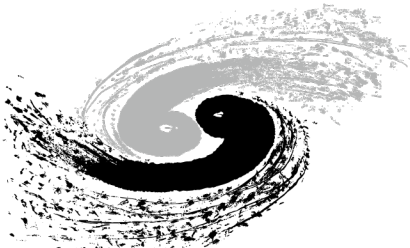


Transition-Edge Sensor Development and Application

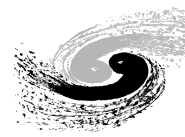
Daikang Yan

2023-10

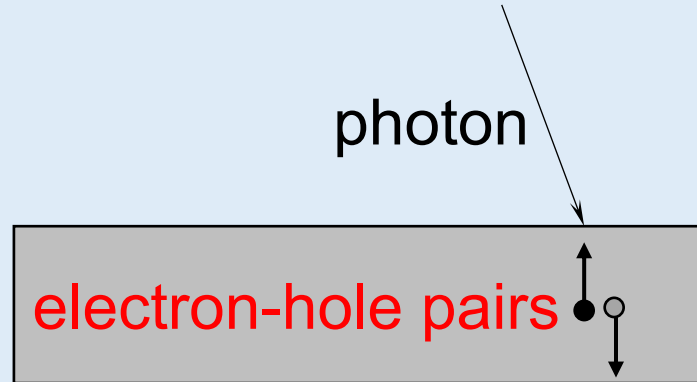


中国科学院高能物理研究所
Institute of High Energy Physics, Chinese Academy of Sciences

Superconductor Detectors



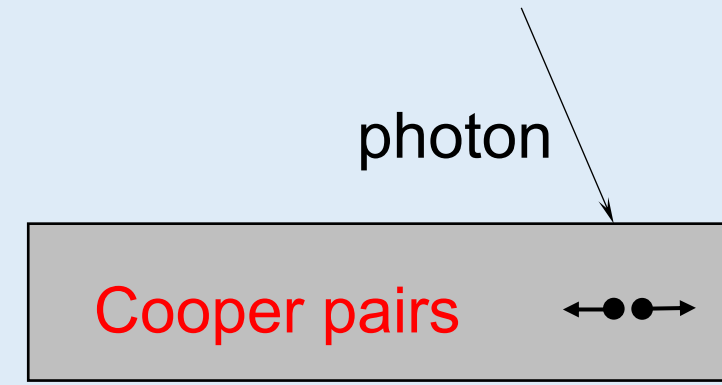
Semiconductor detector



e-h pair: \sim eV

v.s.

Superconductor detector



Cooper pair: \sim meV

$$\text{Poisson noise} = 1/\sqrt{N}$$

The intrinsic noise level of superconductor detectors is $1/\sqrt{1000}$ times lower
 \rightarrow energy resolution 30 times better

Superconductor Detectors

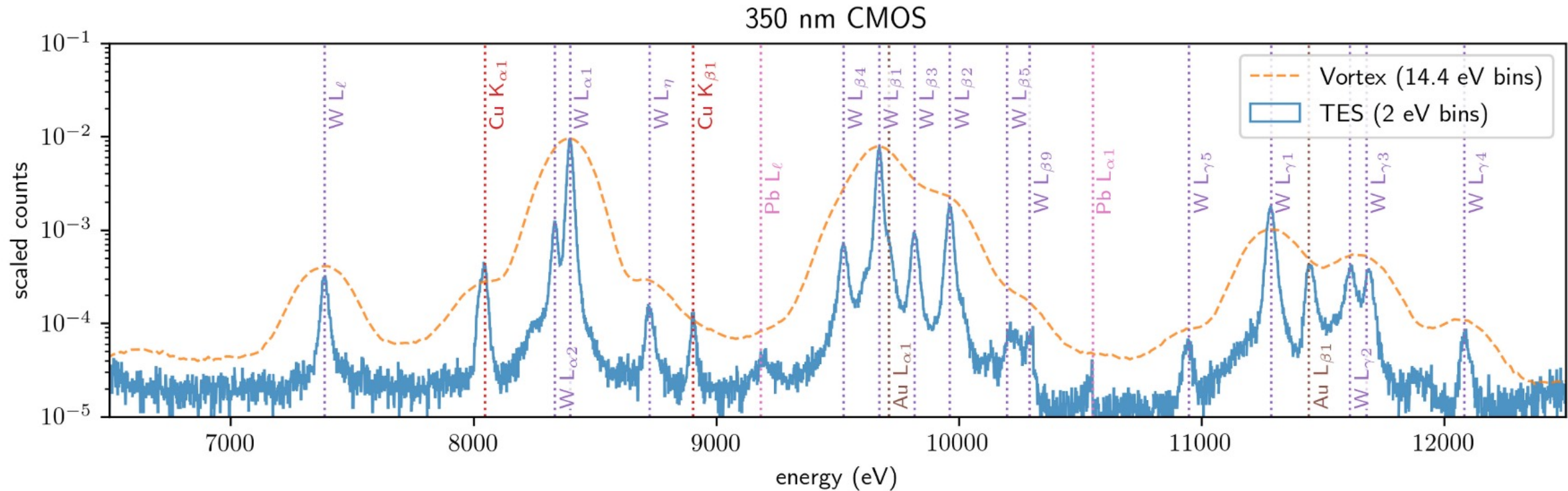


Fig. 3. Fluorescence spectra of a 350 nm CMOS integrated circuit chip, measured with a TES sensor (blue solid line) and a Vortex silicon-drift detector (orange dashed line). Prominent peaks are labeled with their corresponding element and line name.

Tejas Guruswamy et al. (2021)

Vortex (Si detector) $\Delta E = 130$ eV

TES (Superconductor detector) $\Delta E = 12 \sim 15$ eV

Superconductor Detectors

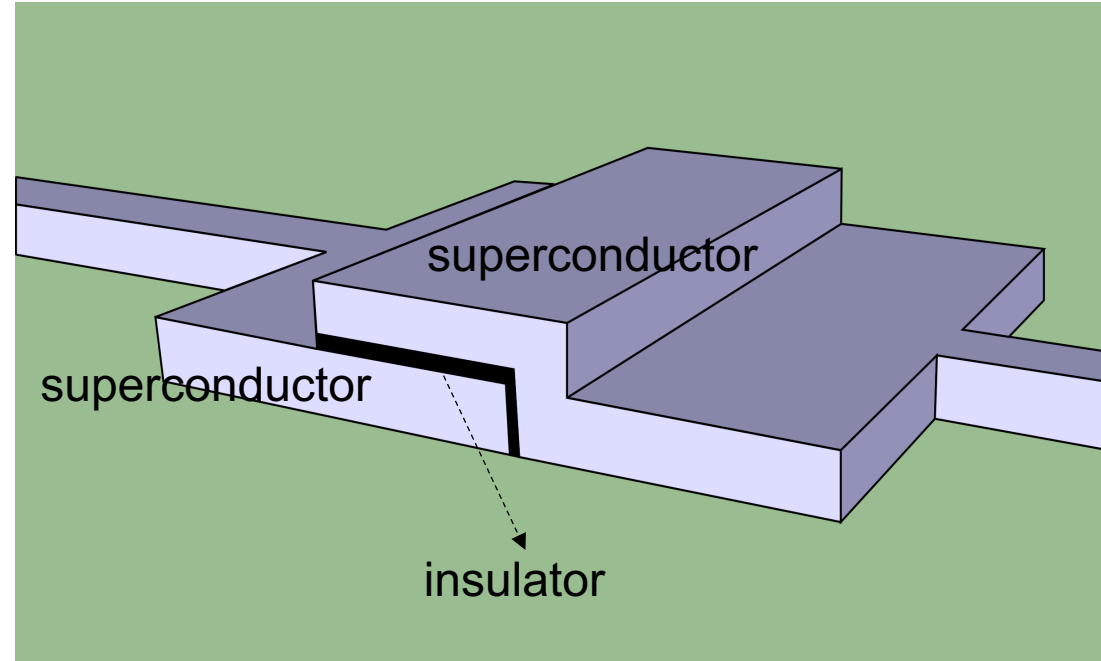


	Superconducting Tunnel Junction (STJ)	Microwave Kinetic Inductance Detectors (MKID)	Metallic Magnetic Calorimeter (MMC)	Transition-Edge Sensor (TES)
mechanism	tunnelling current proportional to number of quasiparticles	quasiparticle density influences the resonant frequency of LC circuit	magnetic flux change in the paramagnetic material	resistance change due to photon heating
ΔE (soft X-ray)	~ 10 eV	\sim several 10 eV	~ 1 eV	~ 1 eV
ΔE (hard X-ray)	detector material too thin, low absorption	rarely developed	40 eV@60 keV (can be better)	5 eV @ 17 keV
advantage	high count rate (10^4 /s)	large array multiplexing	high energy resolution; large energy range	high energy resolution; well-developed multiplex technique
disadvantage	“low” energy resolution; small energy range	“low” energy resolution; small energy range	hard to multiplex	energy range smaller than MMC

Superconductor Detectors



	Superconducting Tunnel Junction (STJ)
mechanism	tunnelling current proportional to number of quasiparticles
ΔE (soft X-ray)	~ 10 eV
ΔE (hard X-ray)	detector material too thin, low absorption
advantage	high count rate (10^4 /s)
disadvantage	“low” energy resolution; small energy range



Superconductor Detectors



mechanism

ΔE
(soft X-ray)

ΔE
(hard X-ray)

advantage

disadvantage

Microwave Kinetic Inductance Detectors (MKID)

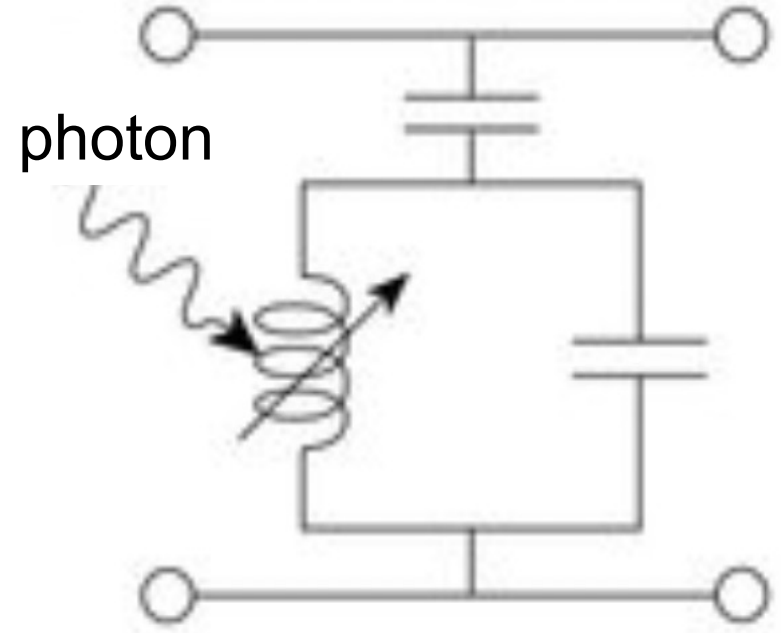
quasiparticle density influences the resonant frequency of LC circuit

~ several 10 eV

rarely developed

large array multiplexing

“low” energy resolution;
small energy range



Superconductor Detectors



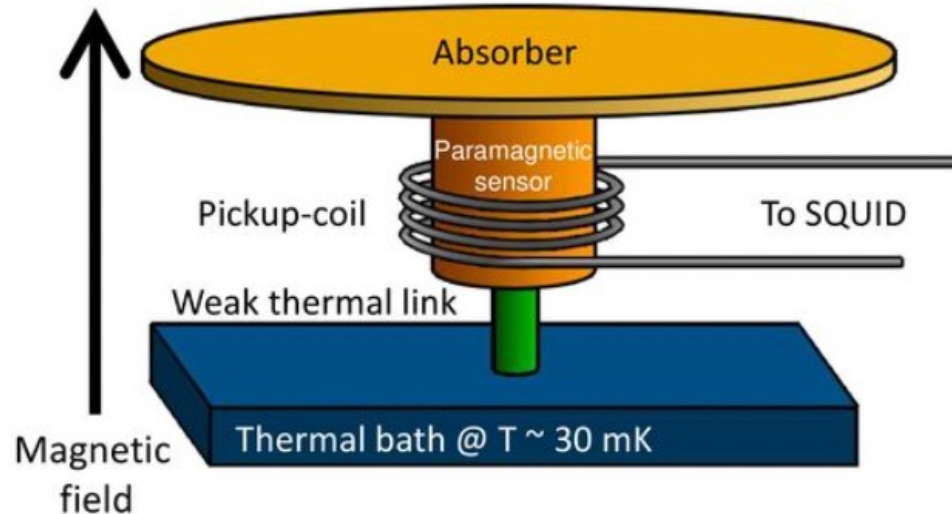
mechanism

ΔE
(soft X-ray)

ΔE
(hard X-ray)

advantage

disadvantage



Metallic Magnetic
Calorimeter
(MMC)

magnetic flux change
in the paramagnetic
material

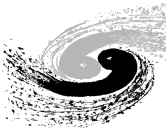
~ 1 eV

40 eV@60 keV
(can be better)

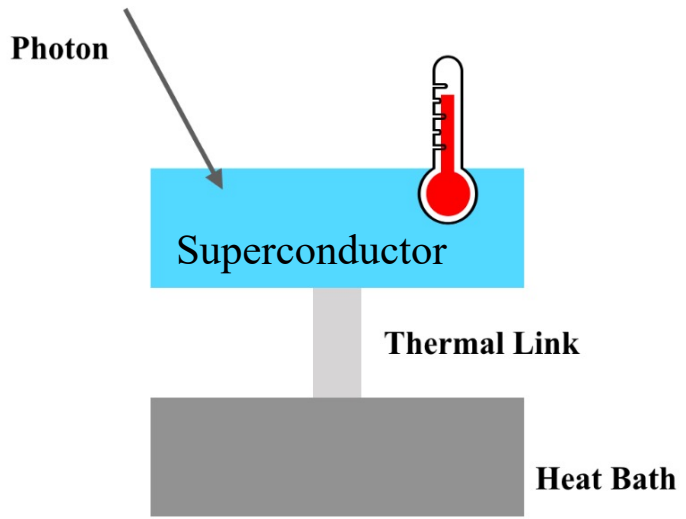
high energy
resolution;
large energy range

hard to multiplex

Superconductor Detectors



mechanism

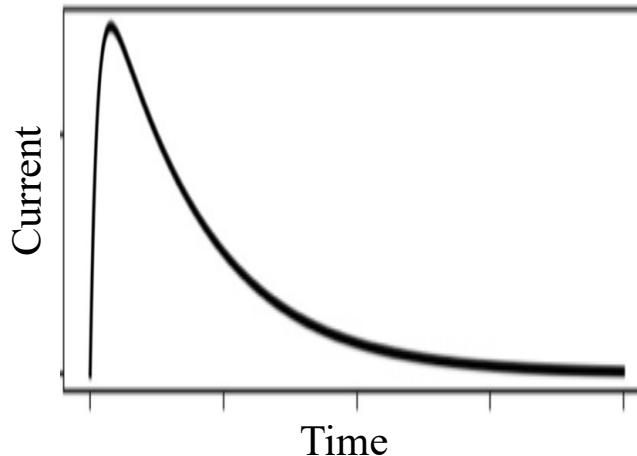
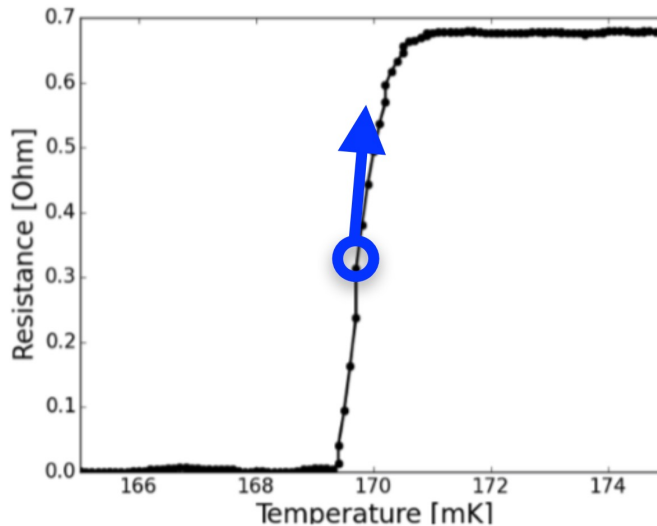
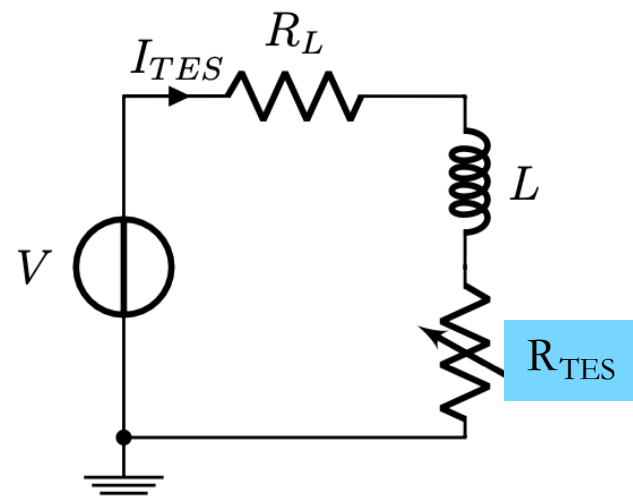


ΔE
(soft X-ray)

ΔE
(hard X-ray)

advantage

disadvantage



Transition-Edge Sensor
(TES)

resistance change due
to photon heating

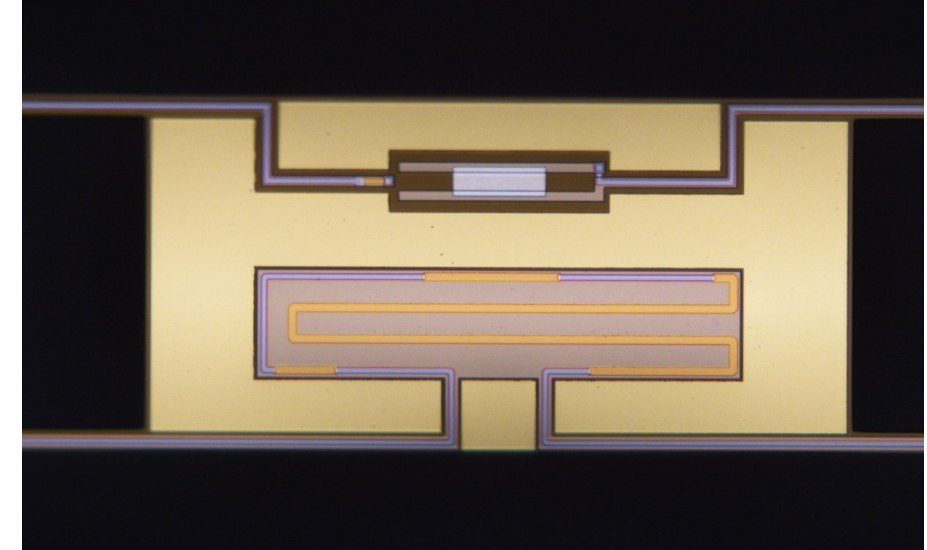
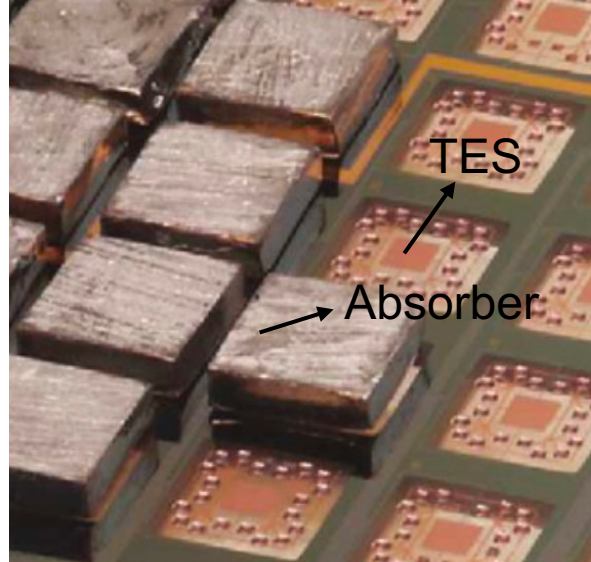
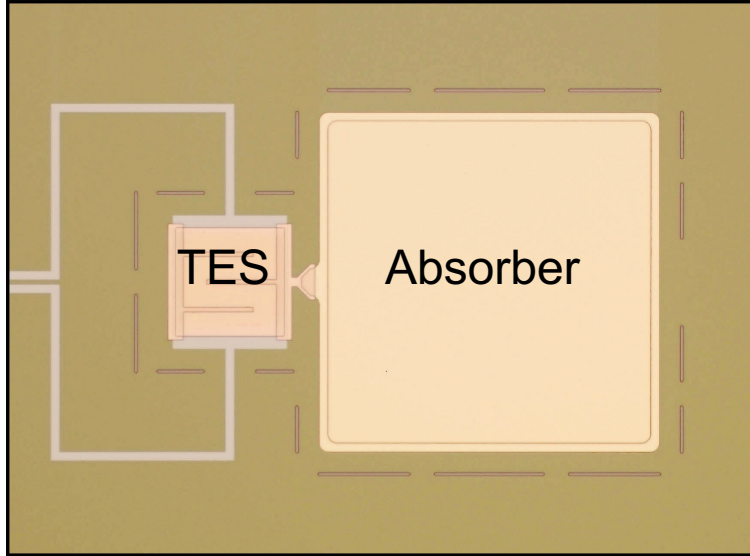
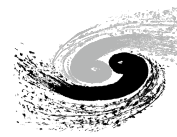
~ 1 eV

5 eV @ 17 keV

high energy resolution;
well-developed multiplex
technique

energy range smaller
than MMC

TES: Transition-Edge Sensor



Bennett *et al.* Rev. Sci. Instrum. **83**, 093113 (2012)

TES: Transition-Edge Sensor

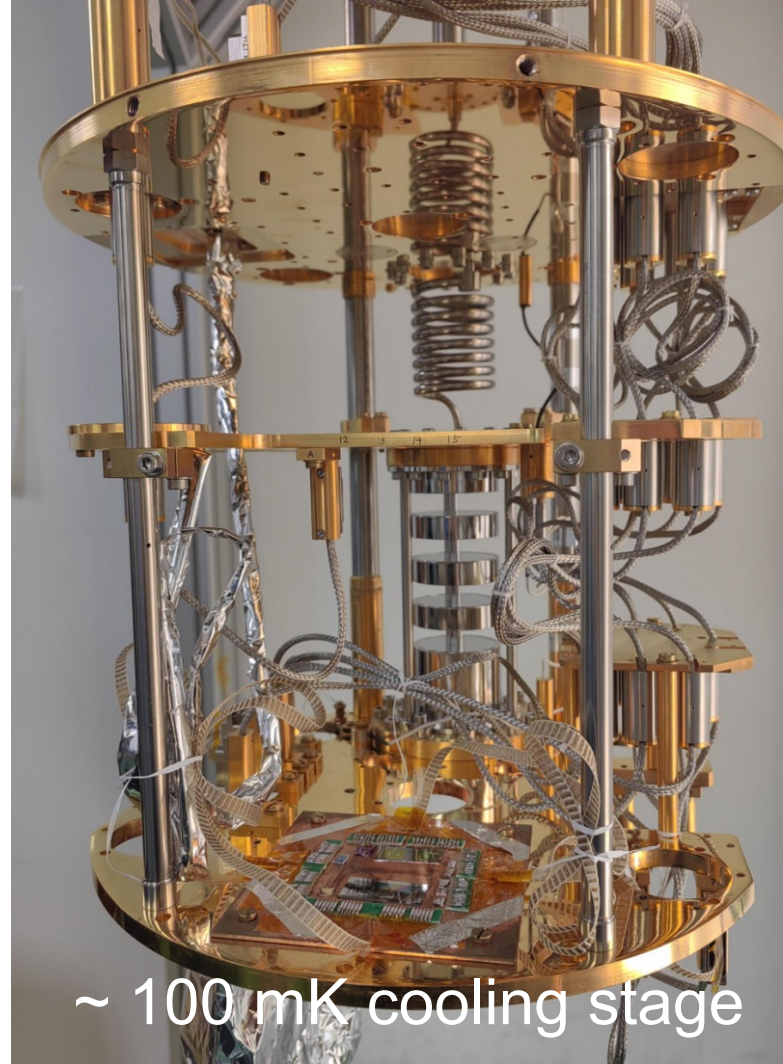
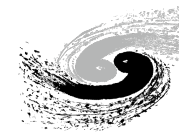


中国科学院高能物理研究所
Institute of High Energy Physics, Chinese Academy of Sciences

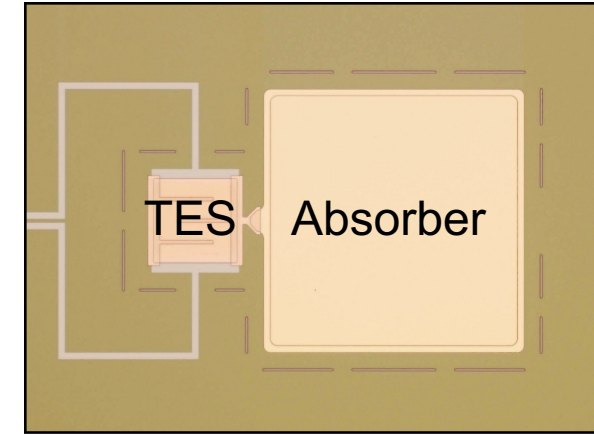
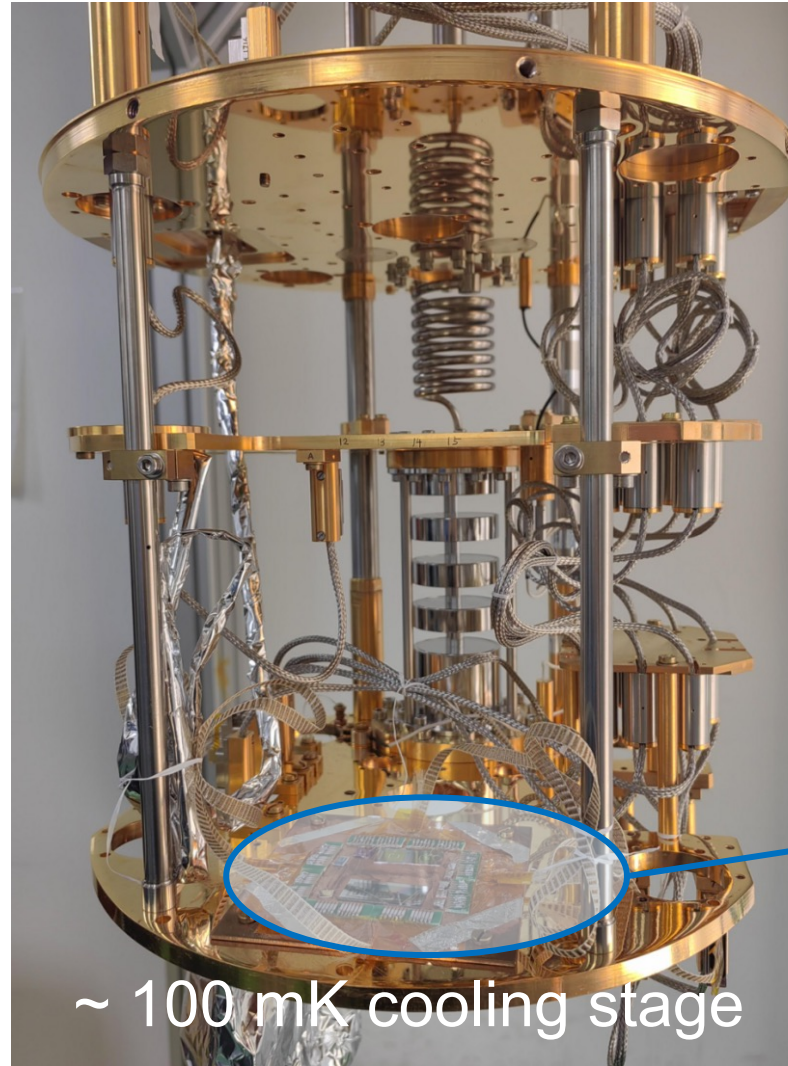
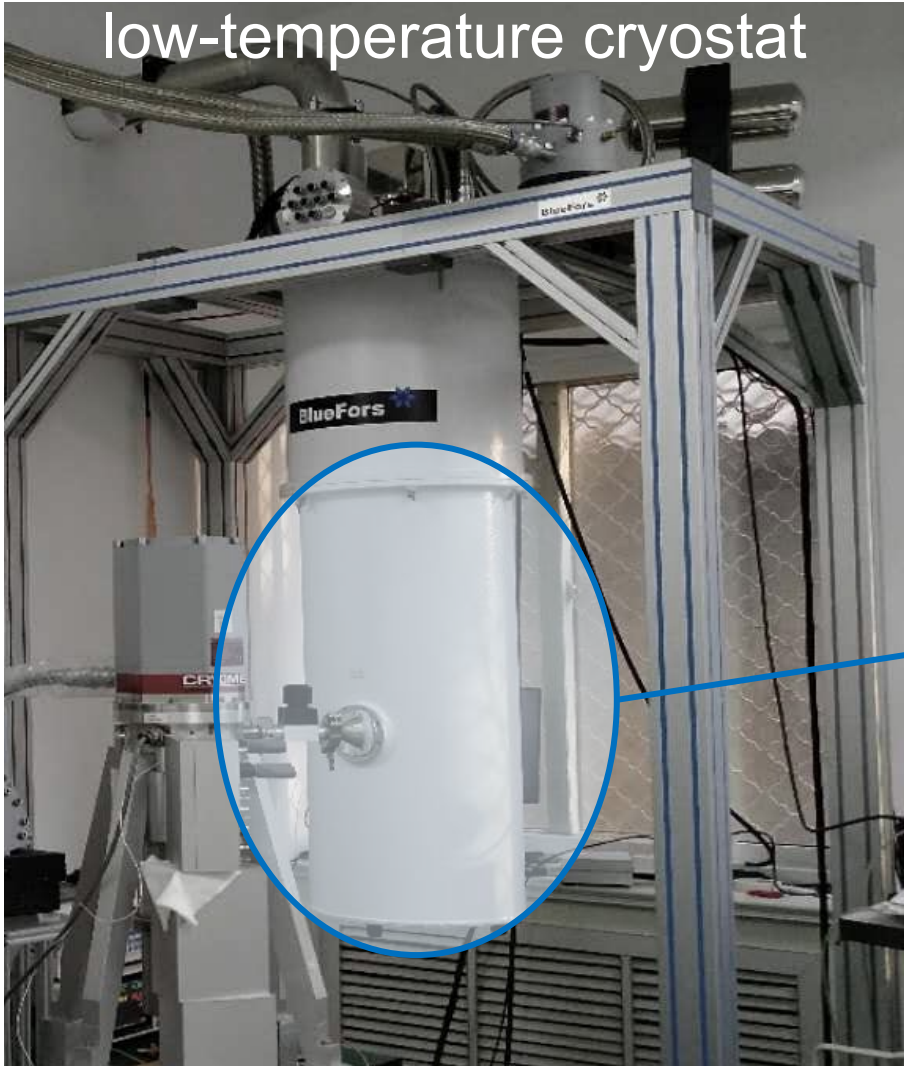
low-temperature cryostat



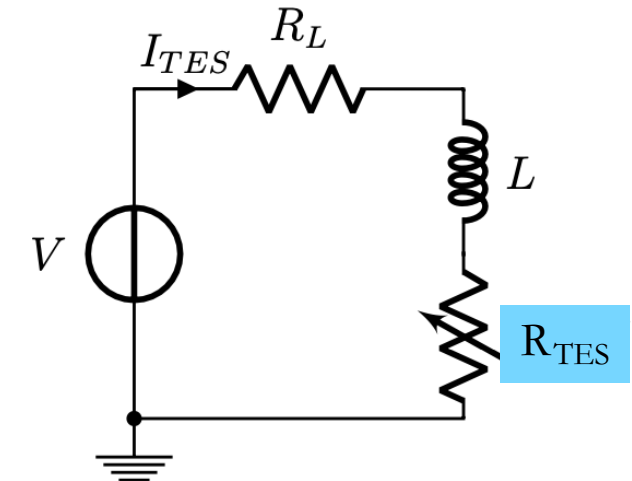
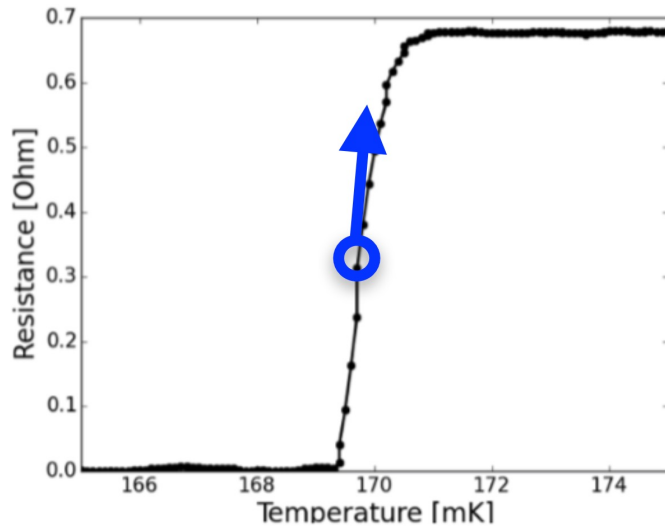
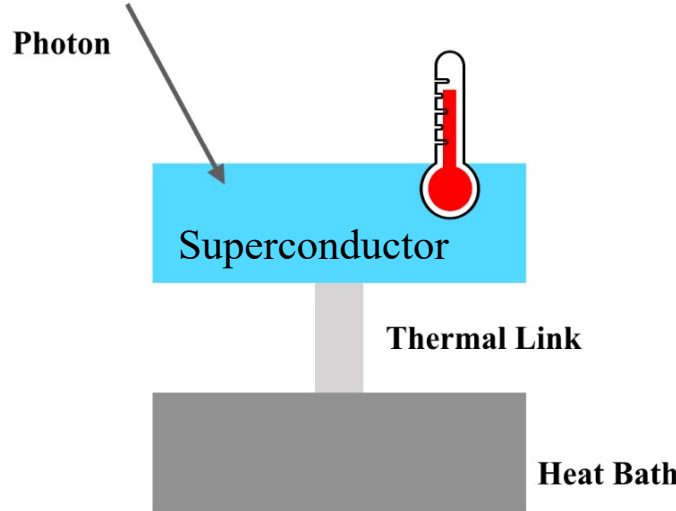
TES: Transition-Edge Sensor



TES: Transition-Edge Sensor



TES Design



Thermal bias

$R(T, I)$ relation

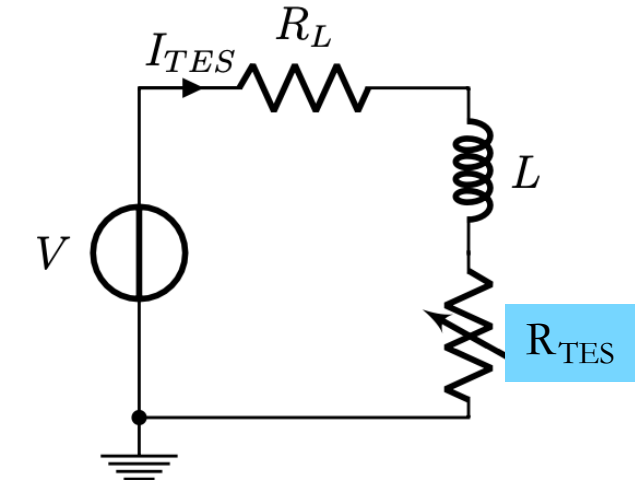
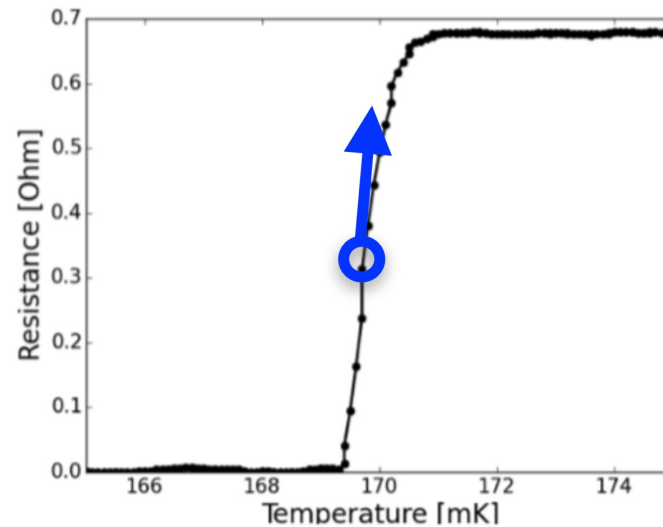
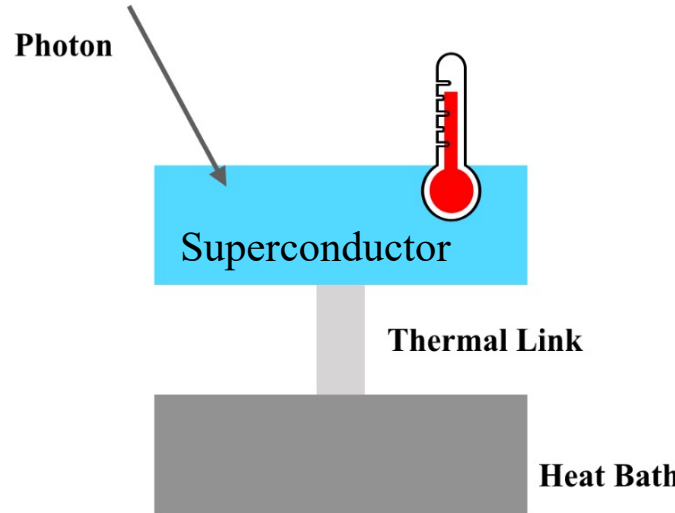
Electrical bias

$$\frac{d\delta T}{dt} = \frac{I_0 R_0 (2 + \beta_I)}{C} \delta I - \frac{(1 - \mathcal{L}_I)}{\tau} \delta T$$

$$R(T, I) \approx R_0 + \alpha_I \frac{R_0}{T_0} \delta T + \beta_I \frac{R_0}{I_0} \delta I$$

$$\frac{d\delta I}{dt} = -\frac{R_L + R_0 (1 + \beta_I)}{L} \delta I - \frac{\mathcal{L}_I G}{I_0 L} \delta T$$

TES Design



Thermal bias

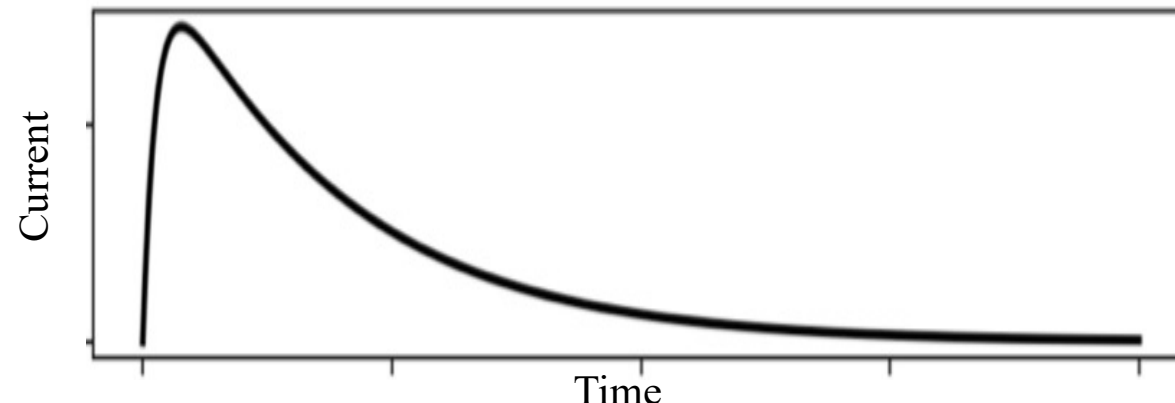
$R(T, I)$ relation

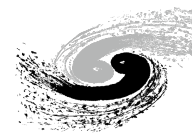
Electrical bias

$$\frac{d\delta T}{dt} = \frac{I_0 R_0 (2 + \beta_I)}{C} \delta I - \frac{(1 - \mathcal{L}_I)}{\tau} \delta T$$

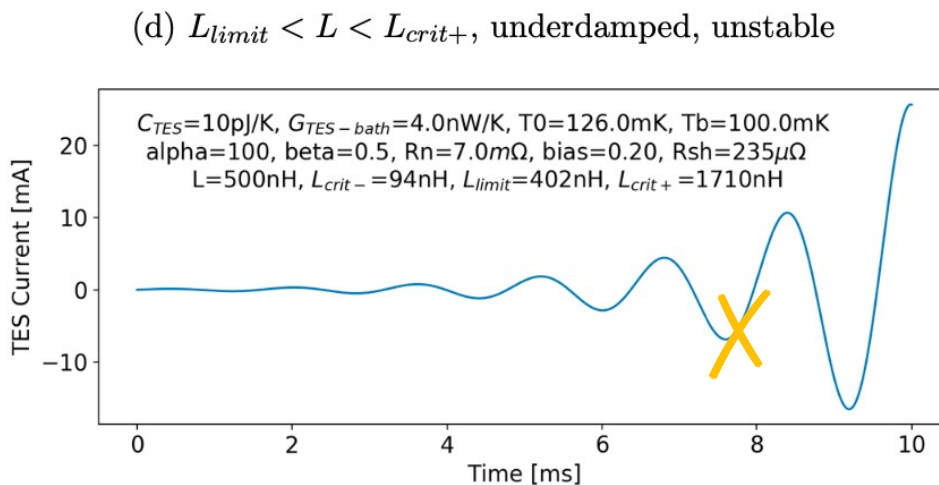
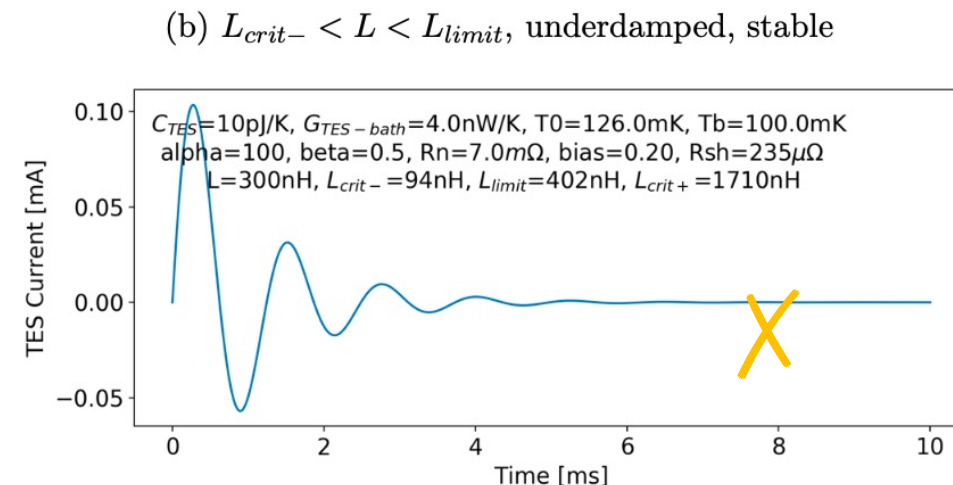
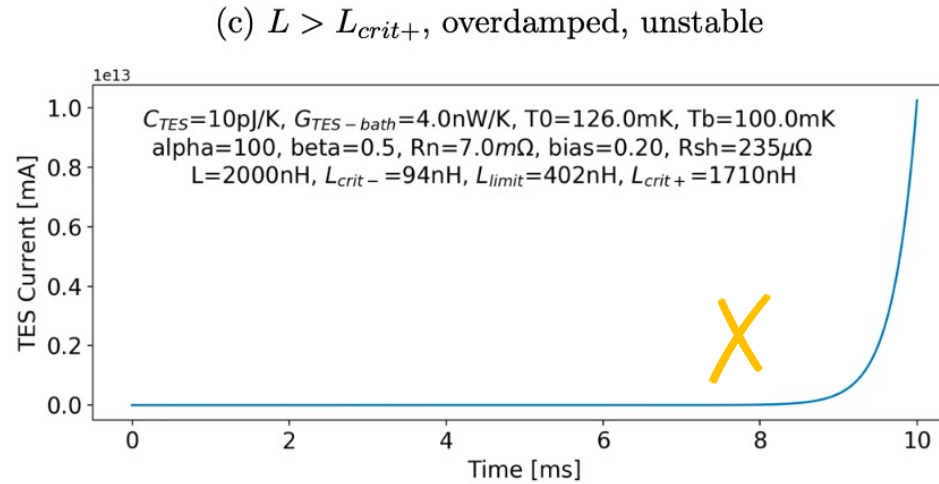
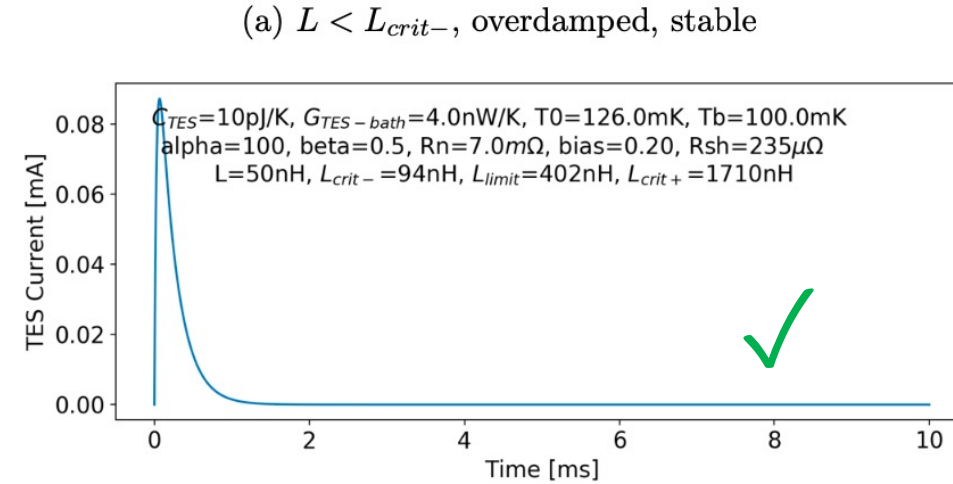
$$R(T, I) \approx R_0 + \alpha_I \frac{R_0}{T_0} \delta T + \beta_I \frac{R_0}{I_0} \delta I$$

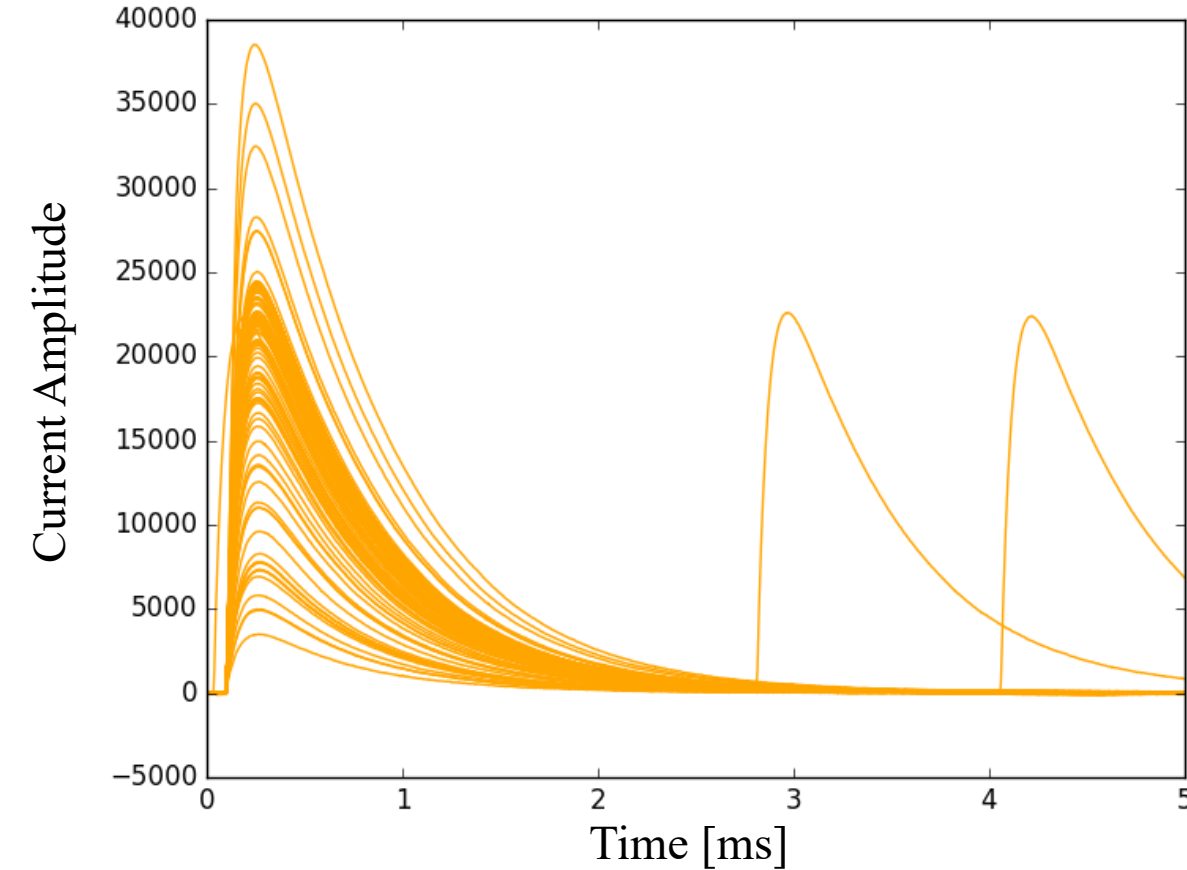
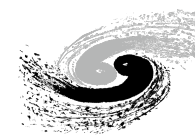
$$\frac{d\delta I}{dt} = -\frac{R_L + R_0 (1 + \beta_I)}{L} \delta I - \frac{\mathcal{L}_I G}{I_0 L} \delta T$$

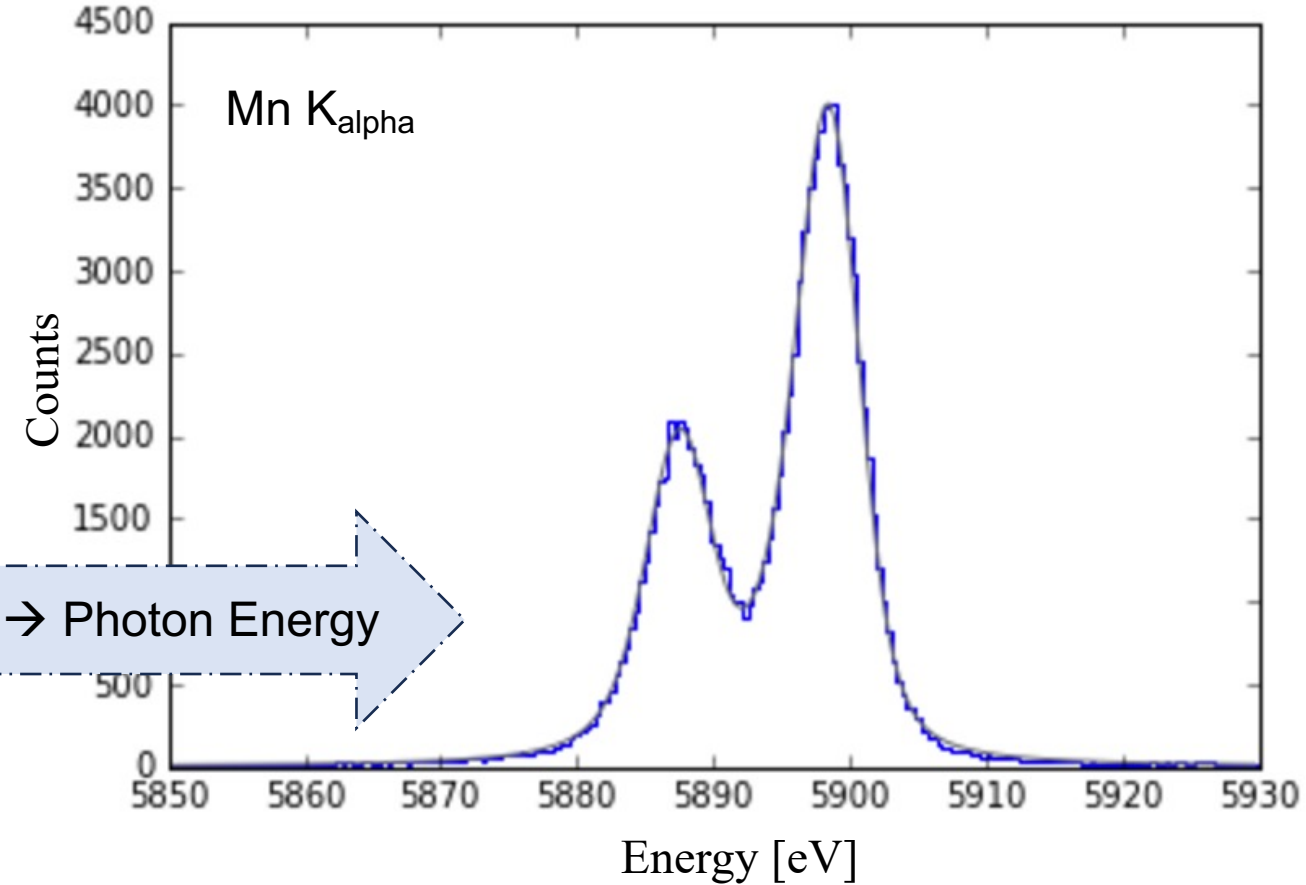
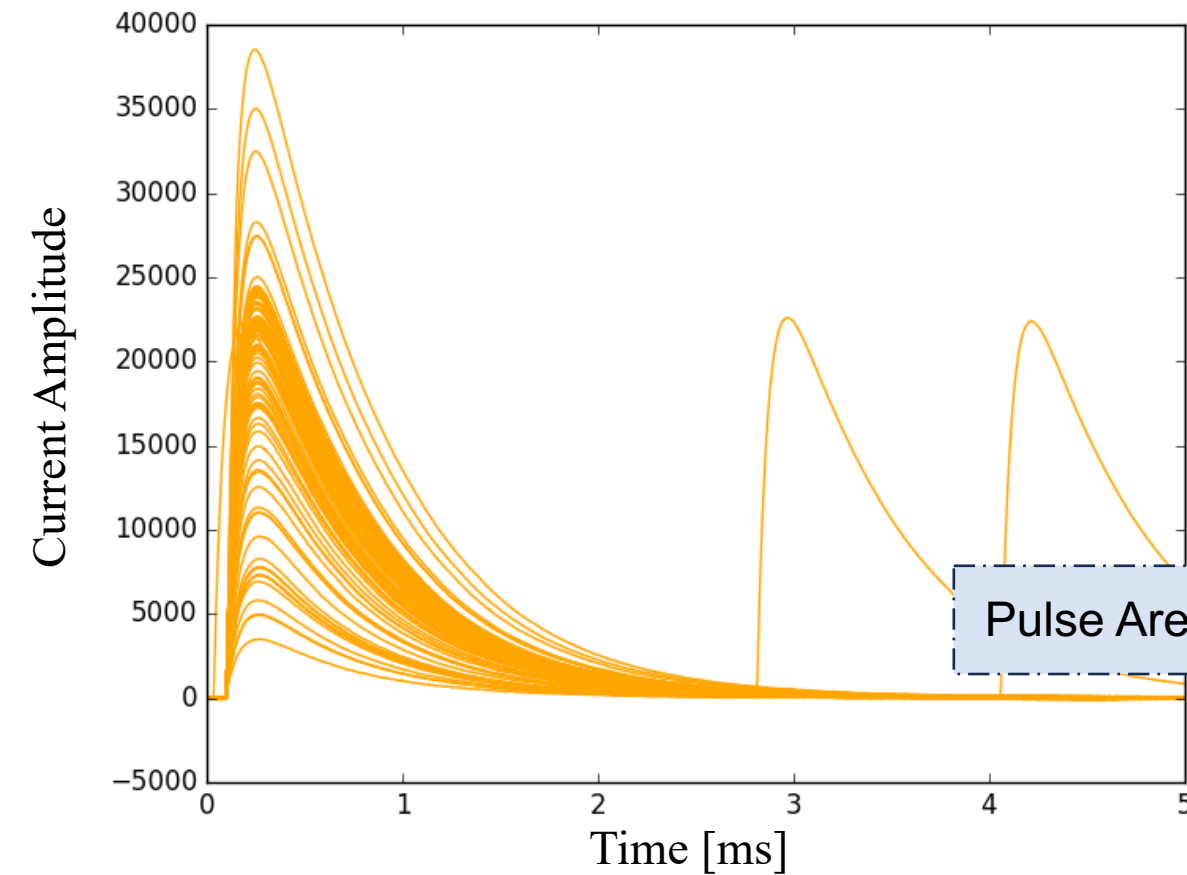




Thermal and electrical parameters should be carefully chosen to produce **stable signal response**







Application I: X-ray Science

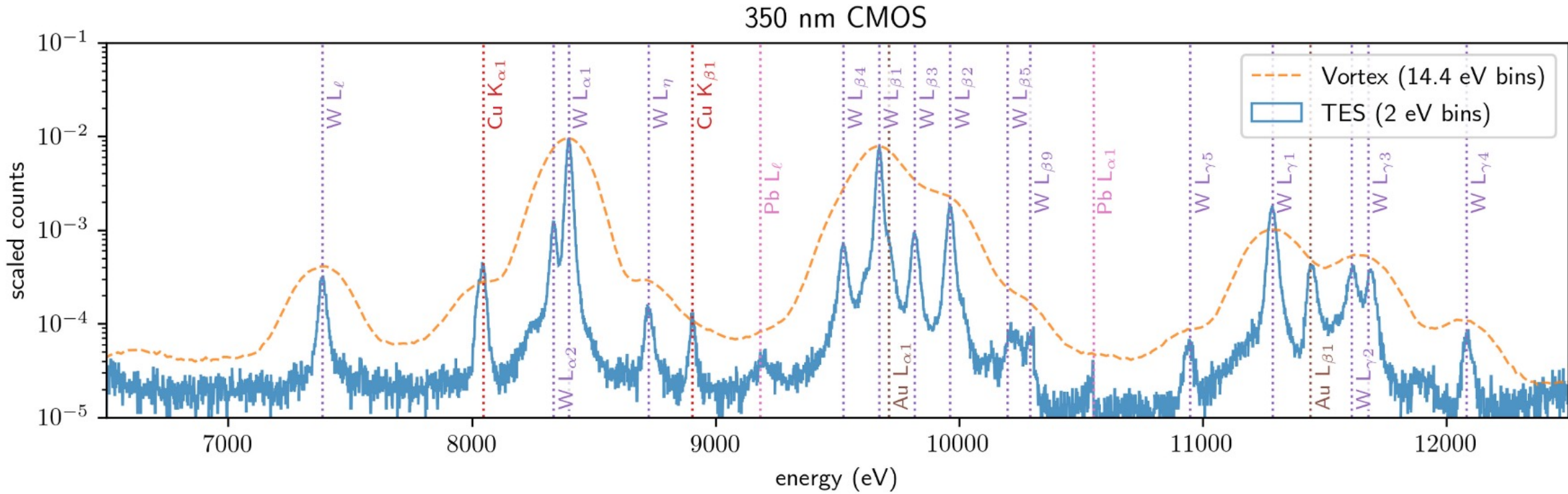
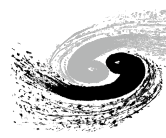


Fig. 3. Fluorescence spectra of a 350 nm CMOS integrated circuit chip, measured with a TES sensor (blue solid line) and a Vortex silicon-drift detector (orange dashed line). Prominent peaks are labeled with their corresponding element and line name.

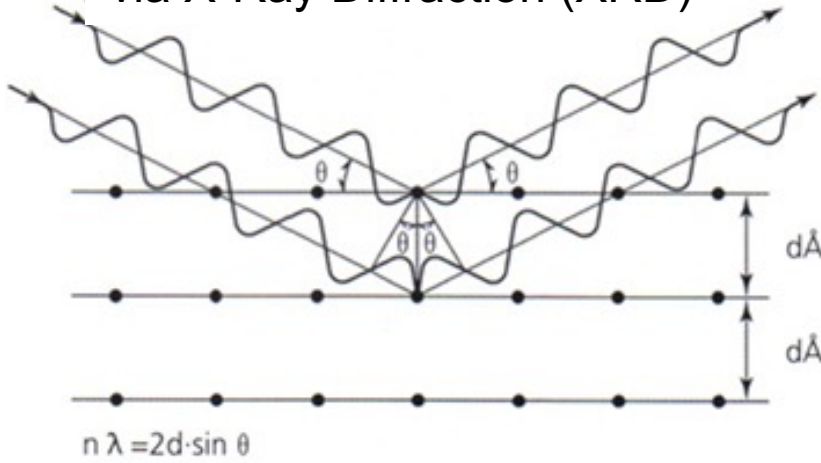
Tejas Guruswamy et al. (2021)

- ✓ neighboring spectral lines
- ✓ low content elements

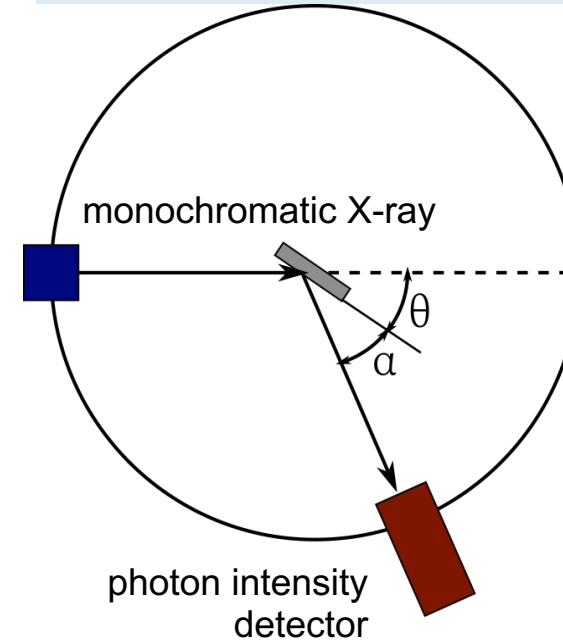
Application I: X-ray Science



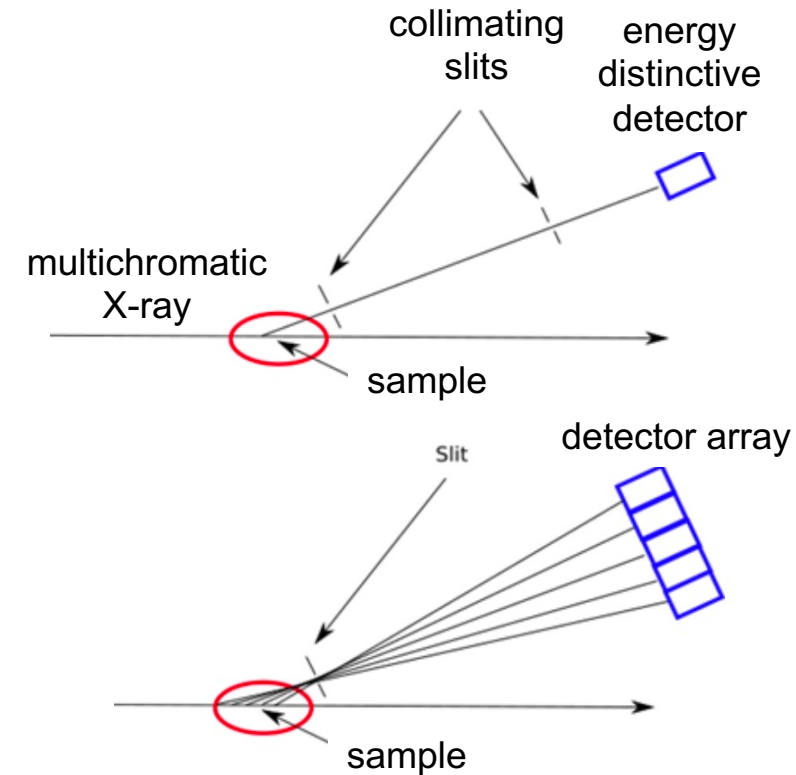
detect crystal structure
via X-Ray Diffraction (XRD)



angular dispersive XRD



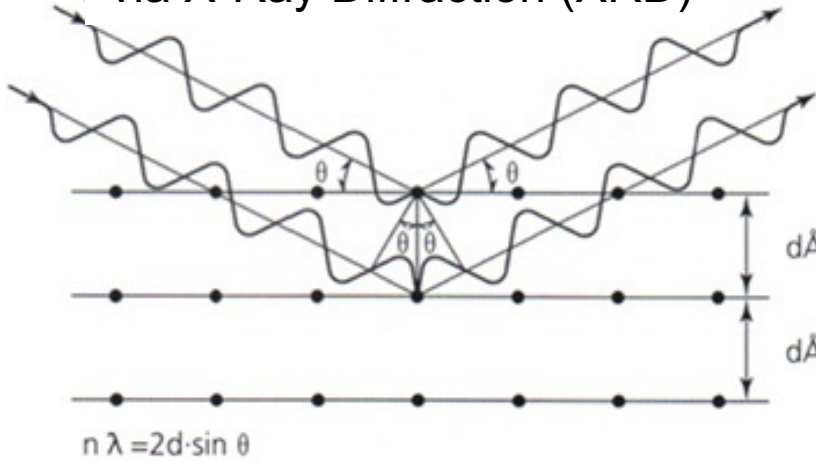
energy dispersive XRD



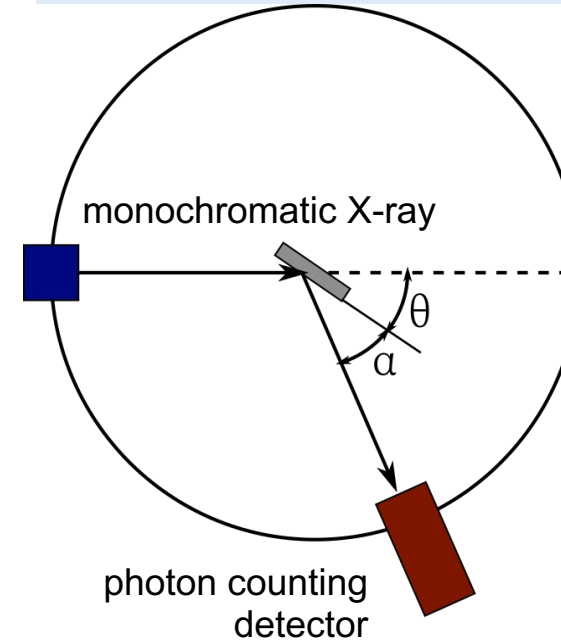
Application I: X-ray Science



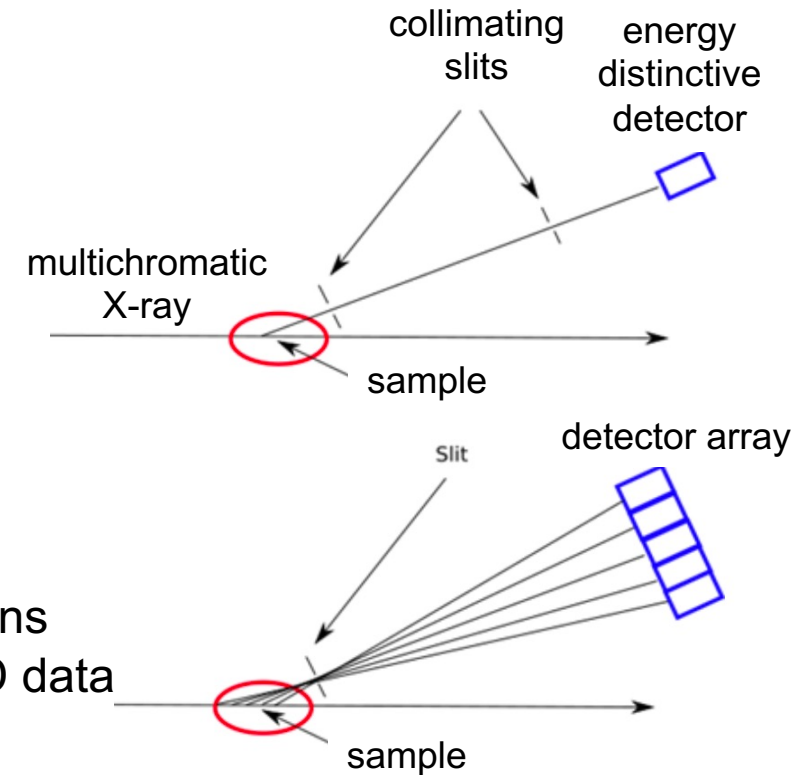
detect crystal structure
via X-Ray Diffraction (XRD)



angular dispersive XRD



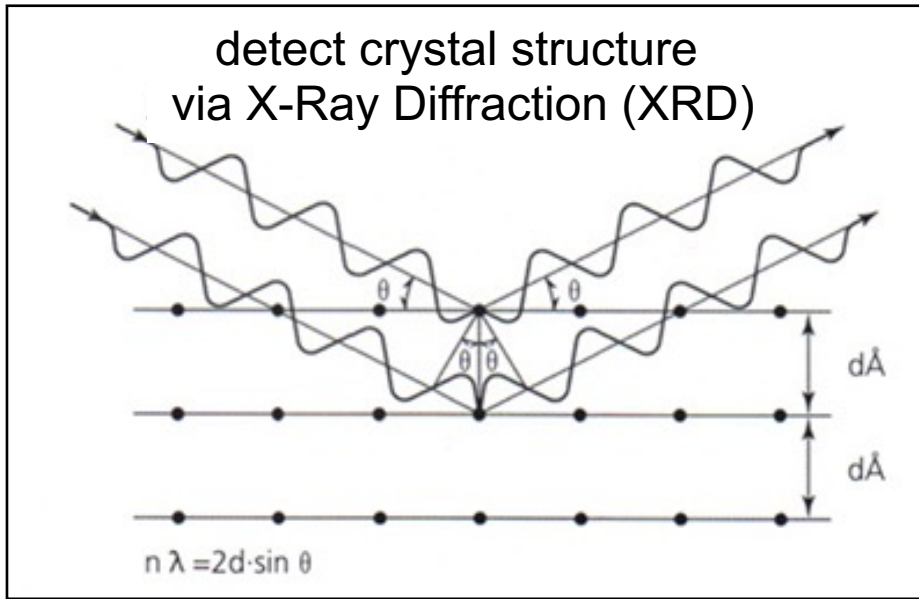
energy dispersive XRD



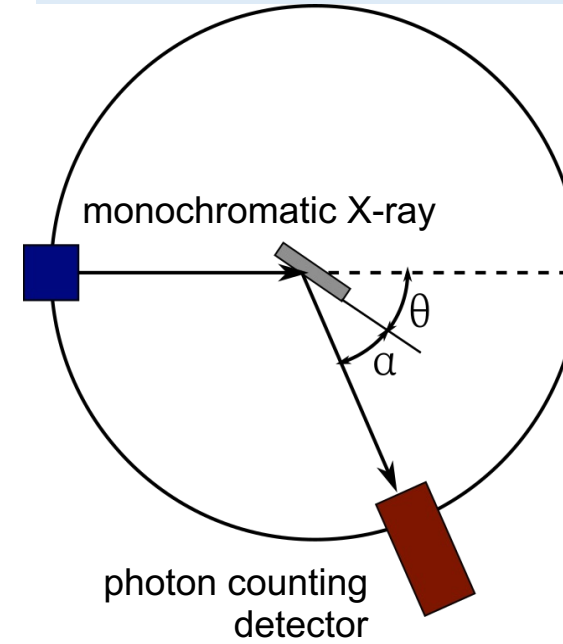
advantage of energy dispersive XRD:

- flexibility: fixed angle, convenient for experiments with extreme conditions
- 2 function in 1 shot: measures characteristic spectra while getting XRD data
- large volume of interest

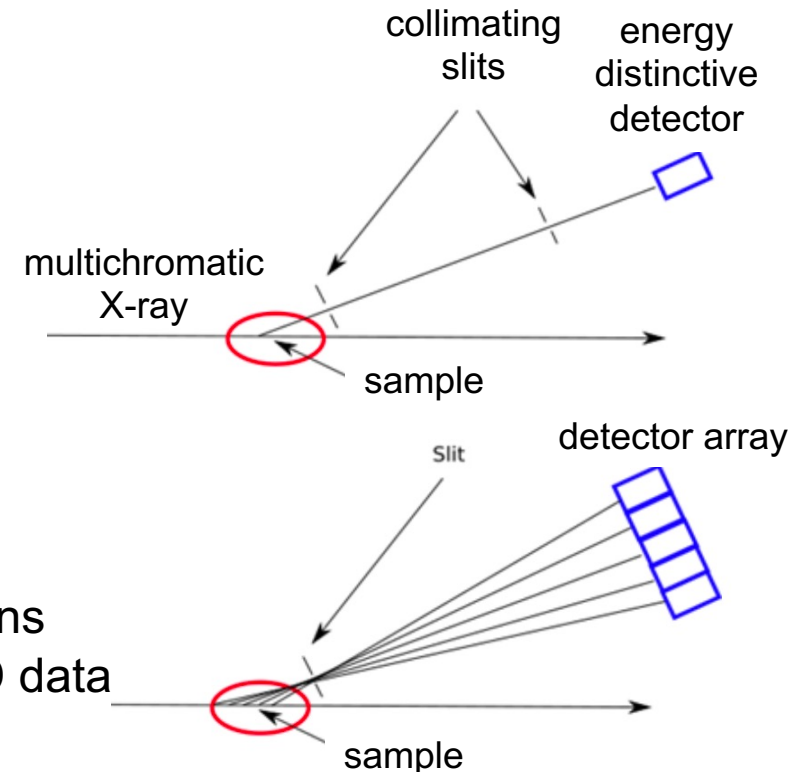
Application I: X-ray Science



angular dispersive XRD



energy dispersive XRD



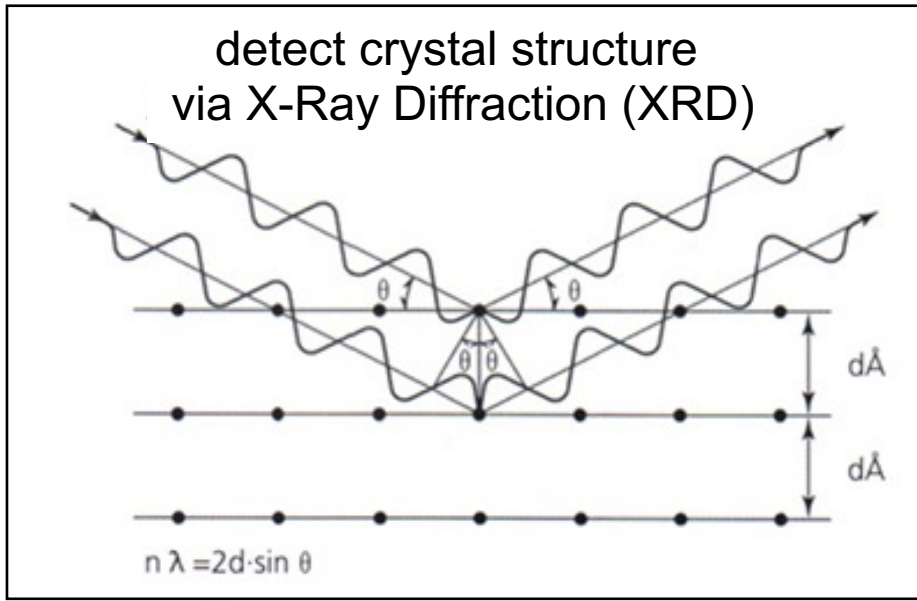
advantage of energy dispersive XRD:

- flexibility: fixed angle, convenient for experiments with extreme conditions
- 2 function in 1 shot: measures characteristic spectra while getting XRD data
- large volume of interest

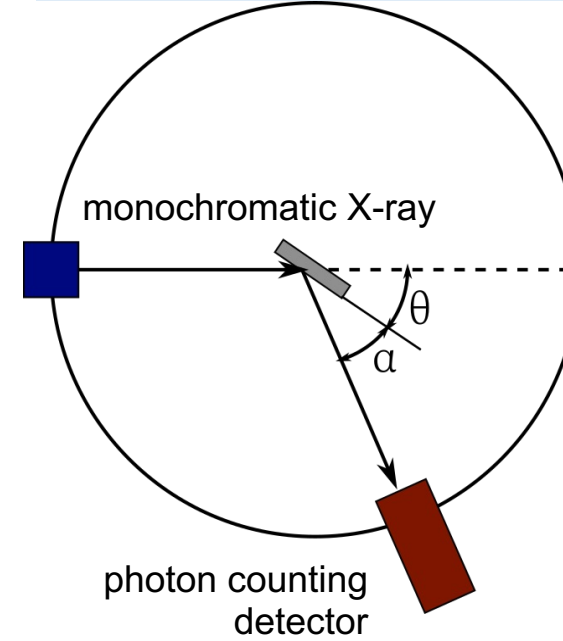
disadvantage:

- resolution worse than angular dispersive XRD with semiconductor detectors (770 eV @ 112 keV)

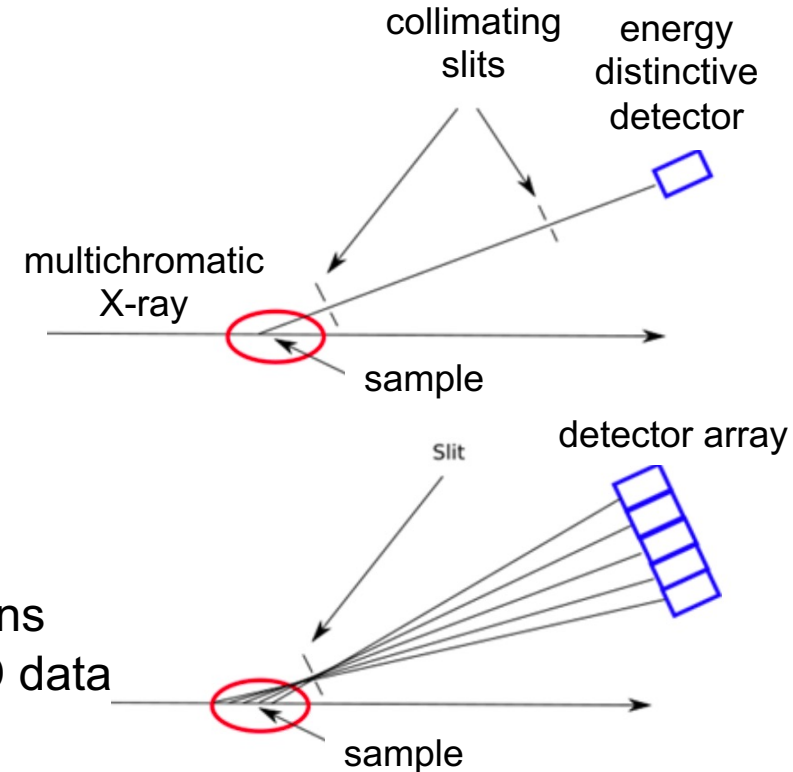
Application I: X-ray Science



angular dispersive XRD



energy dispersive XRD



advantage of energy dispersive XRD:

- flexibility: fixed angle, convenient for experiments with extreme conditions
- 2 function in 1 shot: measures characteristic spectra while getting XRD data
- large volume of interest

disadvantage:

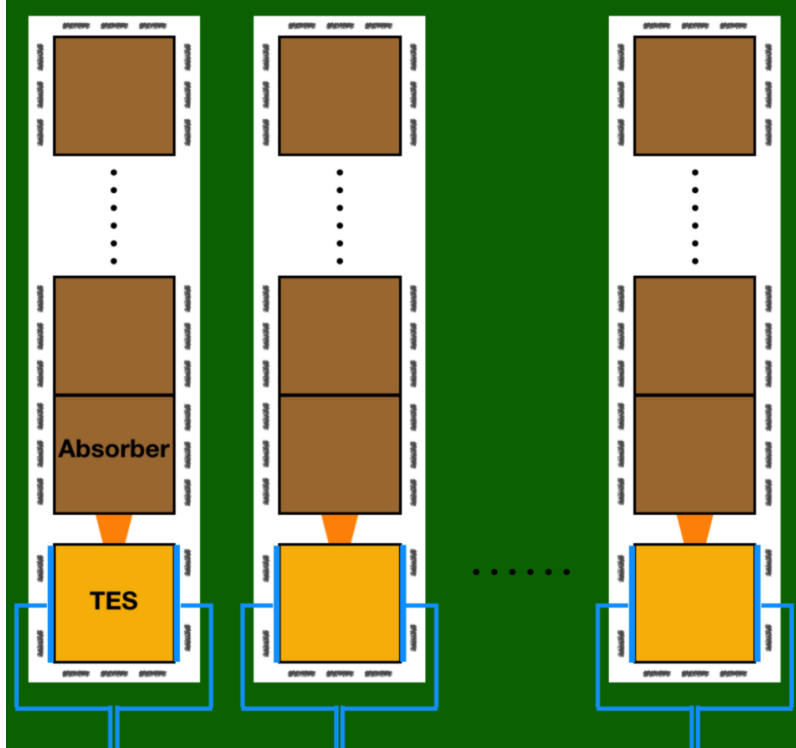
- resolution worse than angular dispersive XRD with semiconductor detectors (770 eV @ 112 keV)

TES detector: 80 eV @ 100 keV, can compete with angular dispersive XRD

Application I: X-ray Science

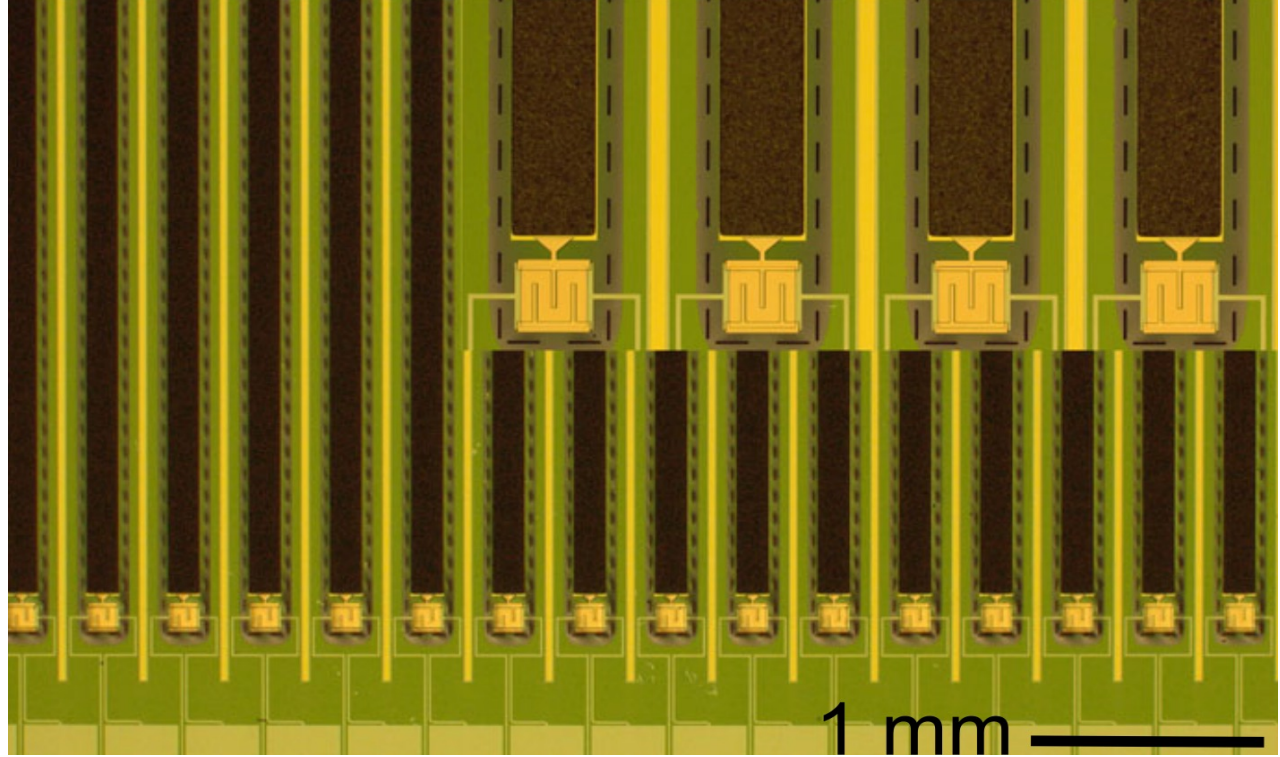


design



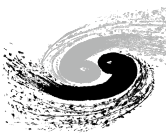
Daikang Yan et al. *IEEE Trans. Appl. Supercond.* 29, 1–4 (2019)

1st version of fabrication

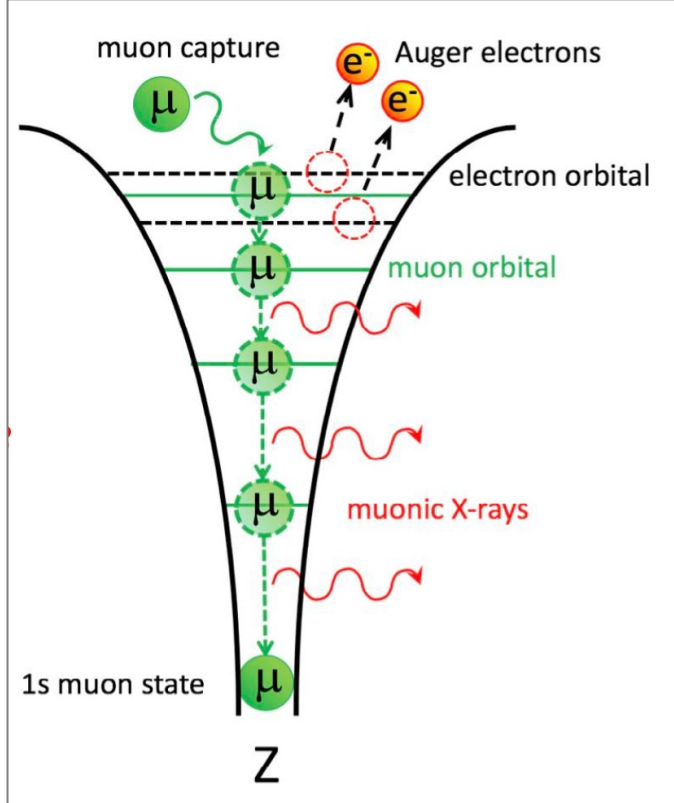


Umeshkumar Patel ... Daikang Yan *J. of Low Temp. Phys.* 199, 384–392 (2020)

Application II: QED



Muon: same charge as an electron, 200 times more massive



Muonic atom Bohr radius: 200 times smaller

Coulomb field: 40,000 times stronger

Study QED (quantum electrodynamics)
under extremely strong electric fields
by
measuring the x-ray energy of
muonic atom de-excitation

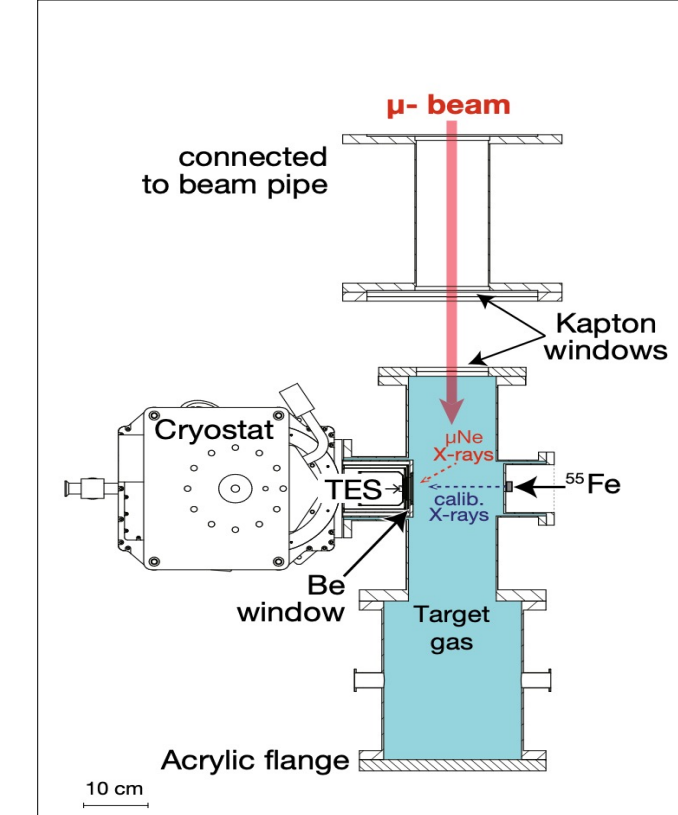
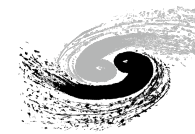


Figure credit: T. Okumura, RIKEN

S. Okada *et al.*, Journal of Low Temperature Physics (2020)
200:445–451

Application II: QED



Target μ -Ar energy:

- 44.3 keV, predicted QED shift 99 eV
- 20.5 keV, predicted QED shift 23 eV

Measurement goal: **measure absolute energy with accuracy of ~ 1 eV**

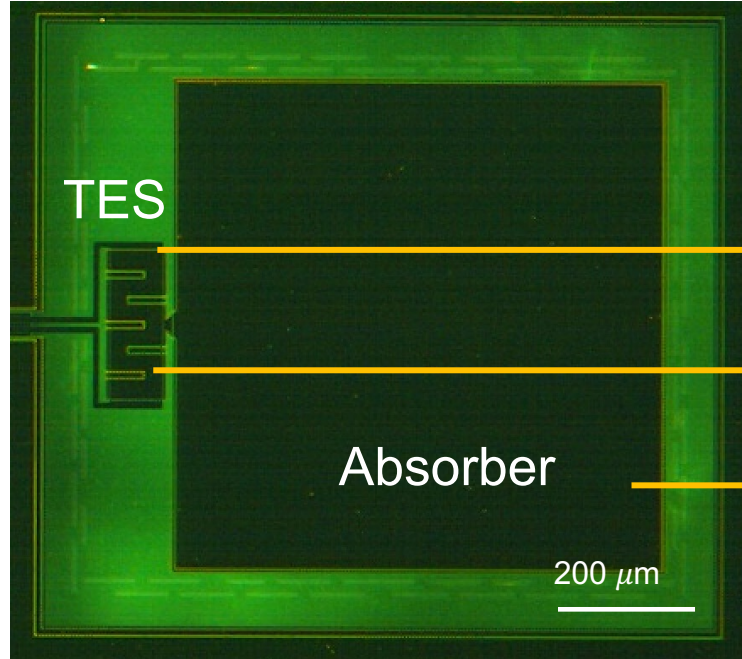
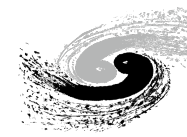


Traditional semiconductor detectors does not have enough **energy resolution** (500 eV @ 45 keV).

TES is a good candidate for this application, the key design considerations are:

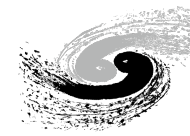
- good linearity under 45 keV $\rightarrow E_{\text{sat}} \propto C/\alpha$
- good energy resolution $\rightarrow \Delta E \propto \sqrt{C/\alpha}$
- high collecting efficiency \rightarrow multiplexing, large absorber

Application II: QED

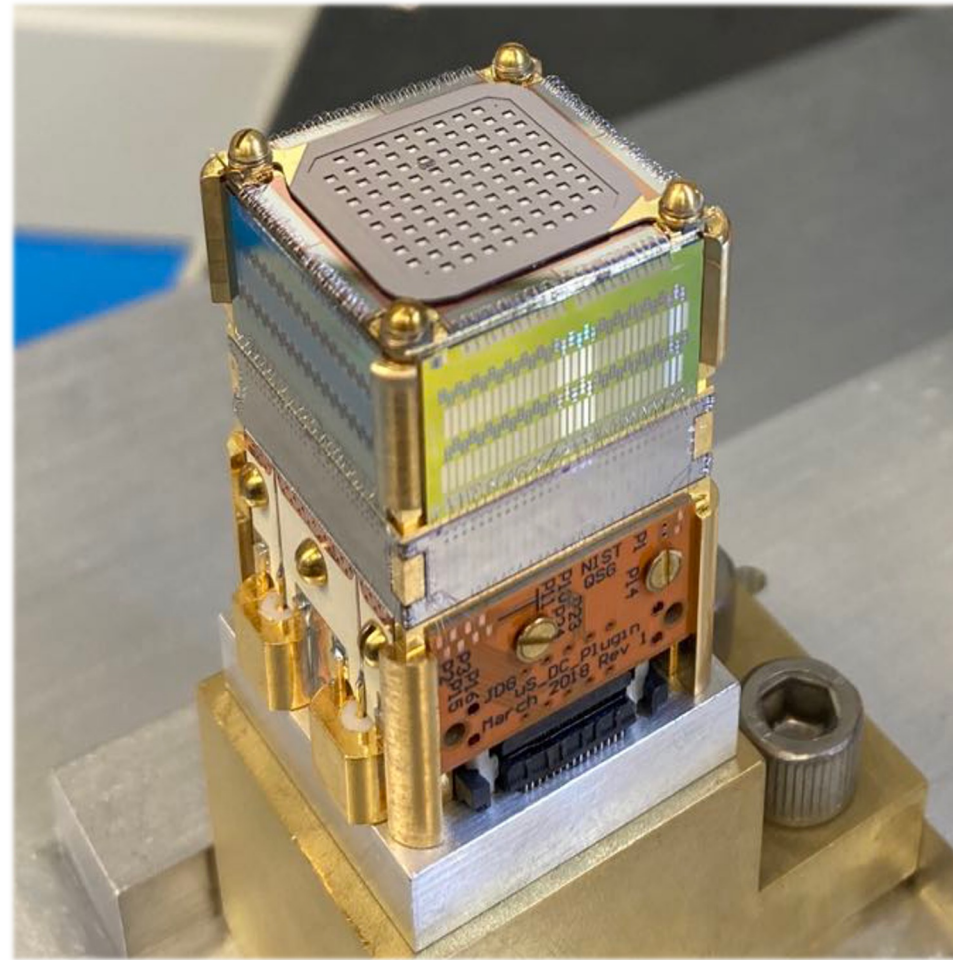


- TES:
Mo/Au bilayer
- Au bars: suppress noise and adjust $\alpha = \frac{\partial \log R}{\partial \log T}$
- Absorber:
Au: large specific heat, set the total **C**
Bi: small specific heat, thick plating to increase **QE**

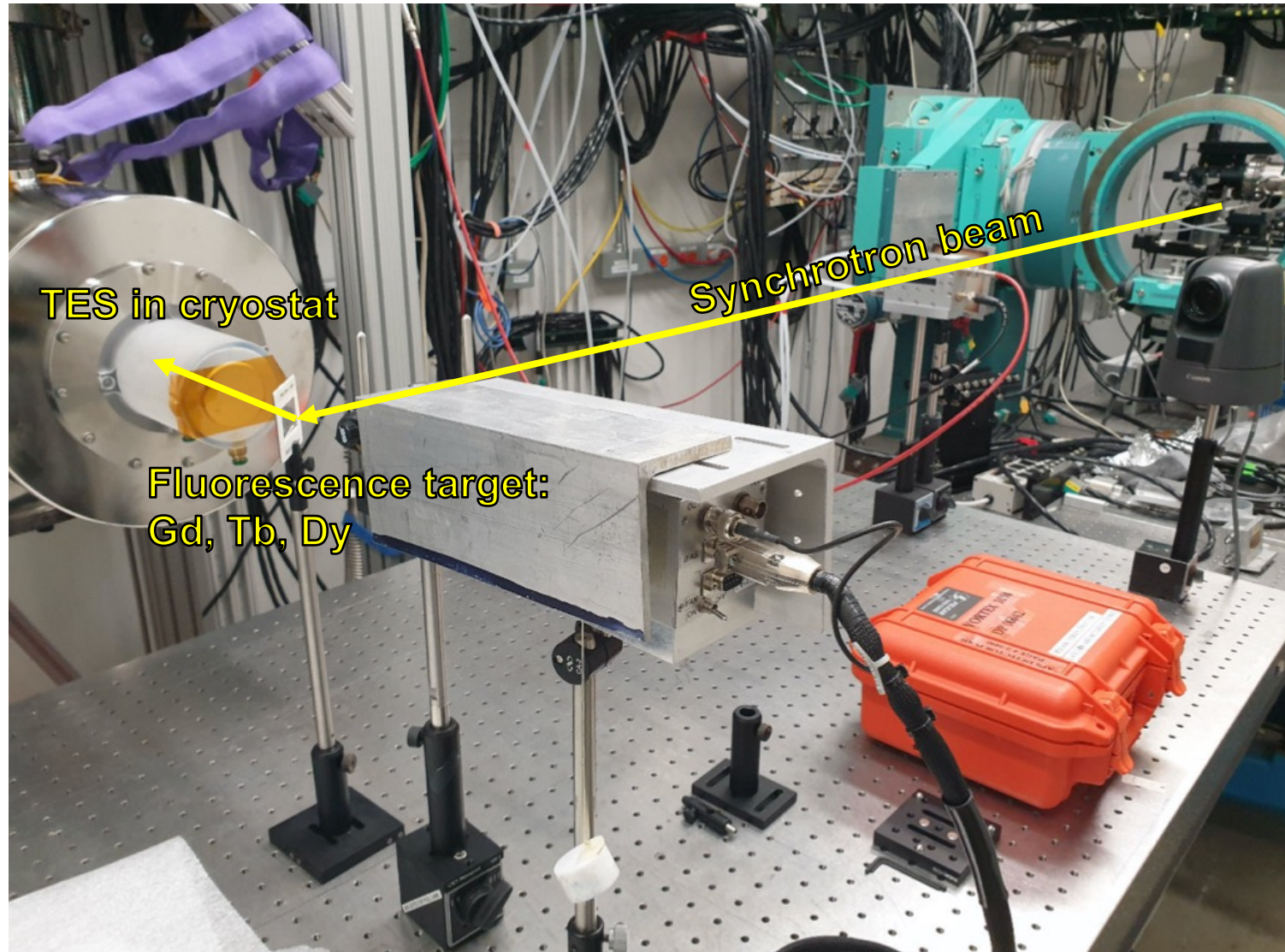
Application II: QED



中國科學院高能物理研究所
Institute of High Energy Physics, Chinese Academy of Sciences



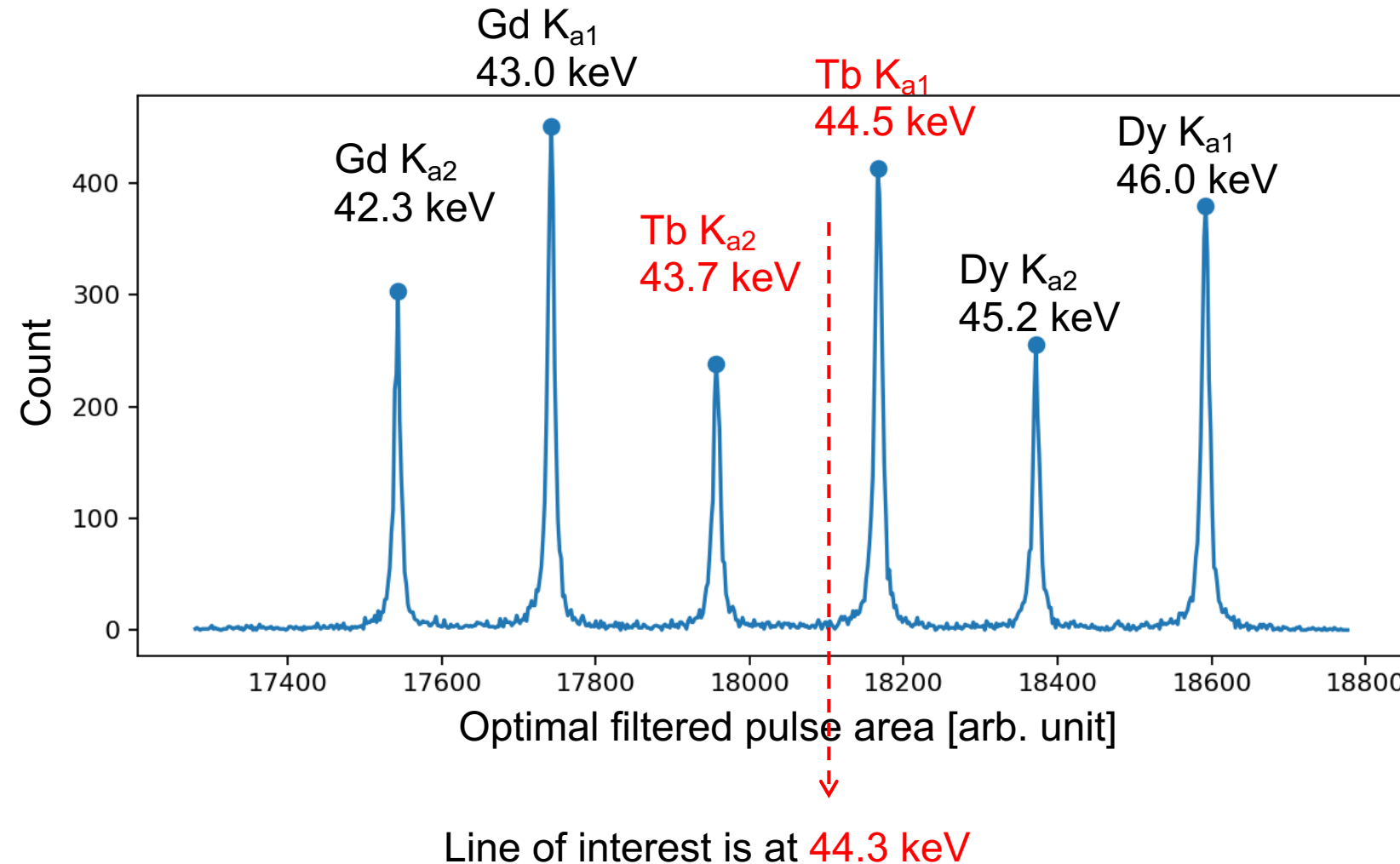
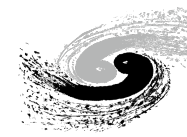
Application II: QED



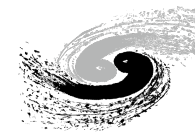
Experiment conducted at Beamline-1BM-C, Advanced Photon Source, ANL, USA

Daikang Yan - IHEP

Application II: QED



Application II: QED

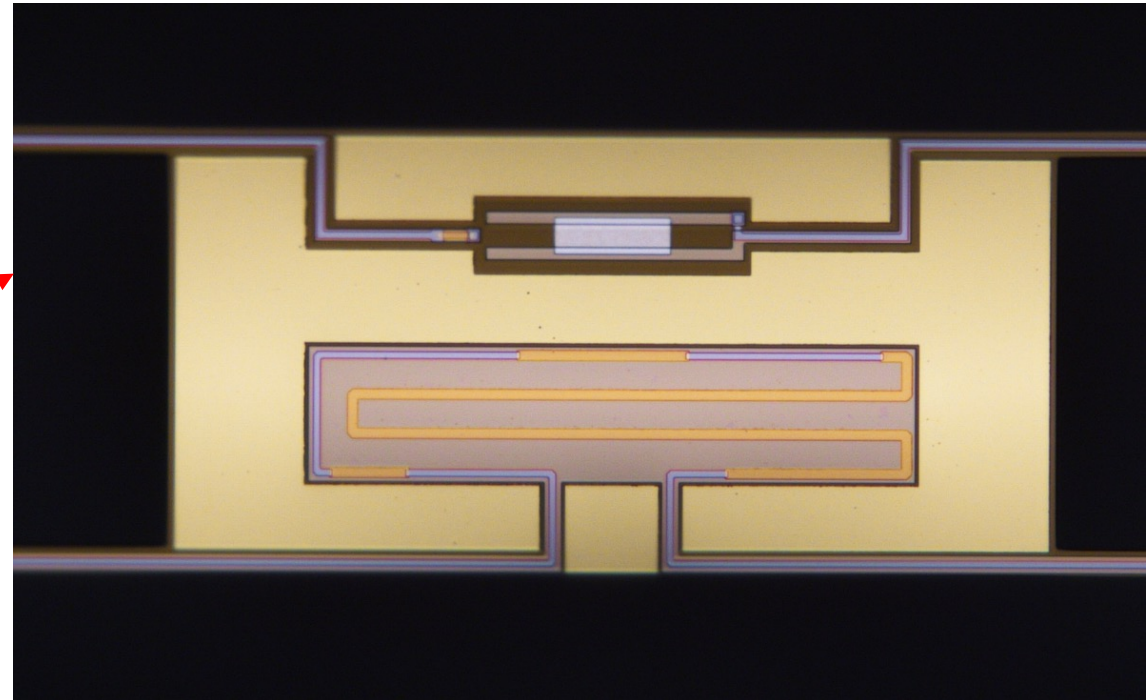
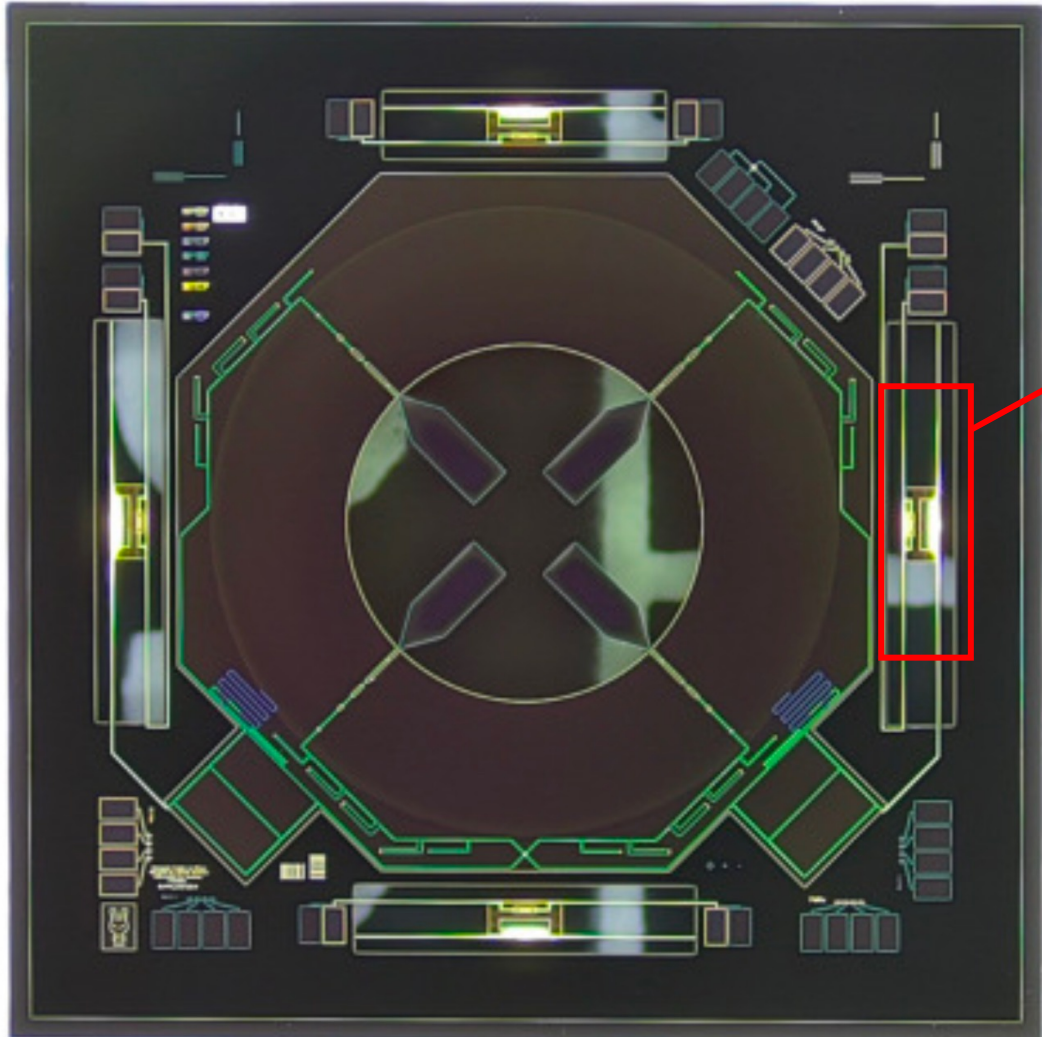


Energy deviation (eV)	Tb K α_1 44.5 keV	Tb K α_2 43.7 keV
5 pJ/K	2.11 (116)	1.00 (122)
6 pJ/K	0.38 (76)	0.13 (84)
7 pJ/K	0.01 (103)	0.24 (107)

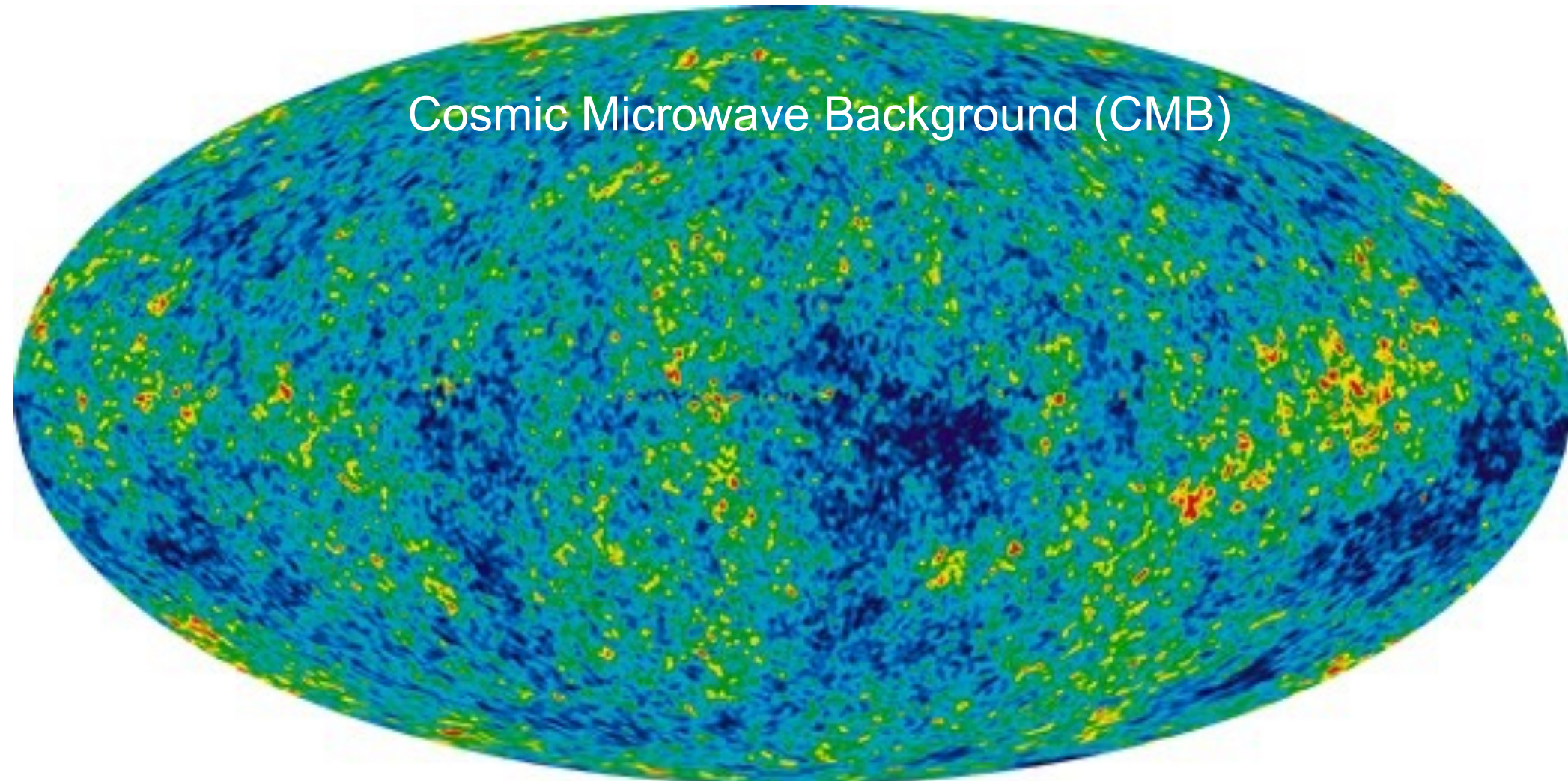
Daikang Yan *et al.* (2022)

More results to come in 2024.....

Application III: Cosmology

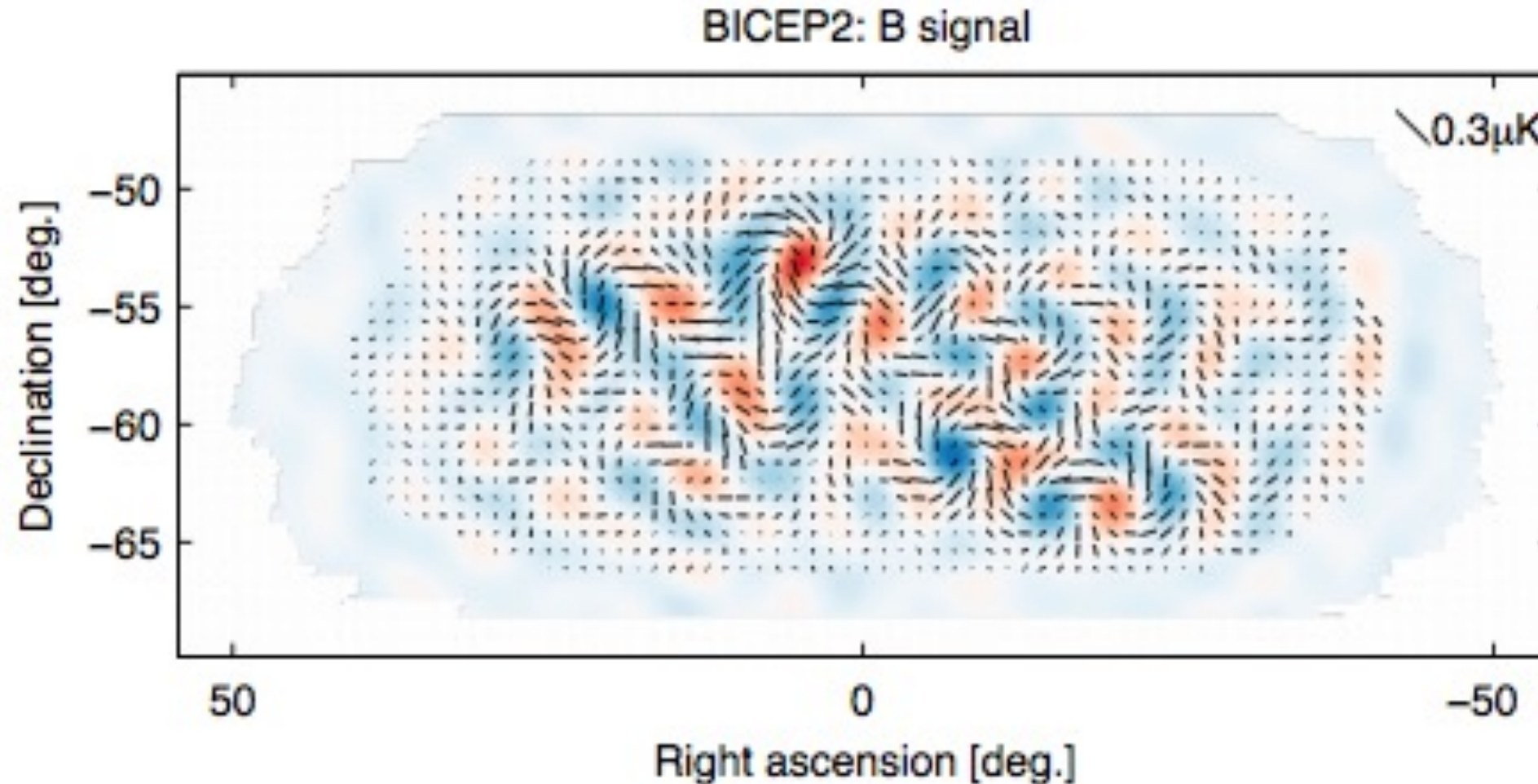


Application III: Cosmology



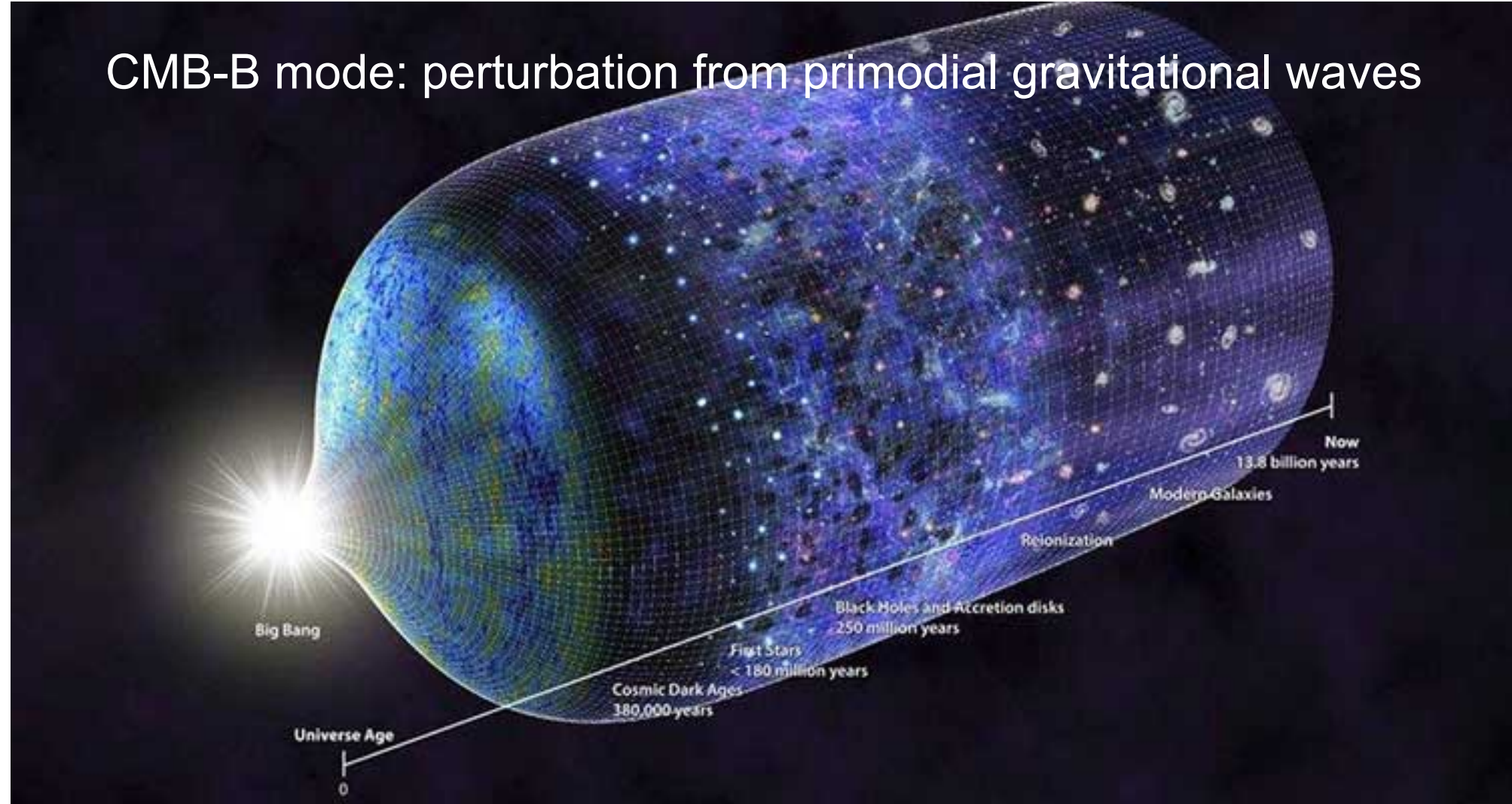
Picture credit: Herbert Huffner, "The Beginning of the World We Know"

Application III: Cosmology



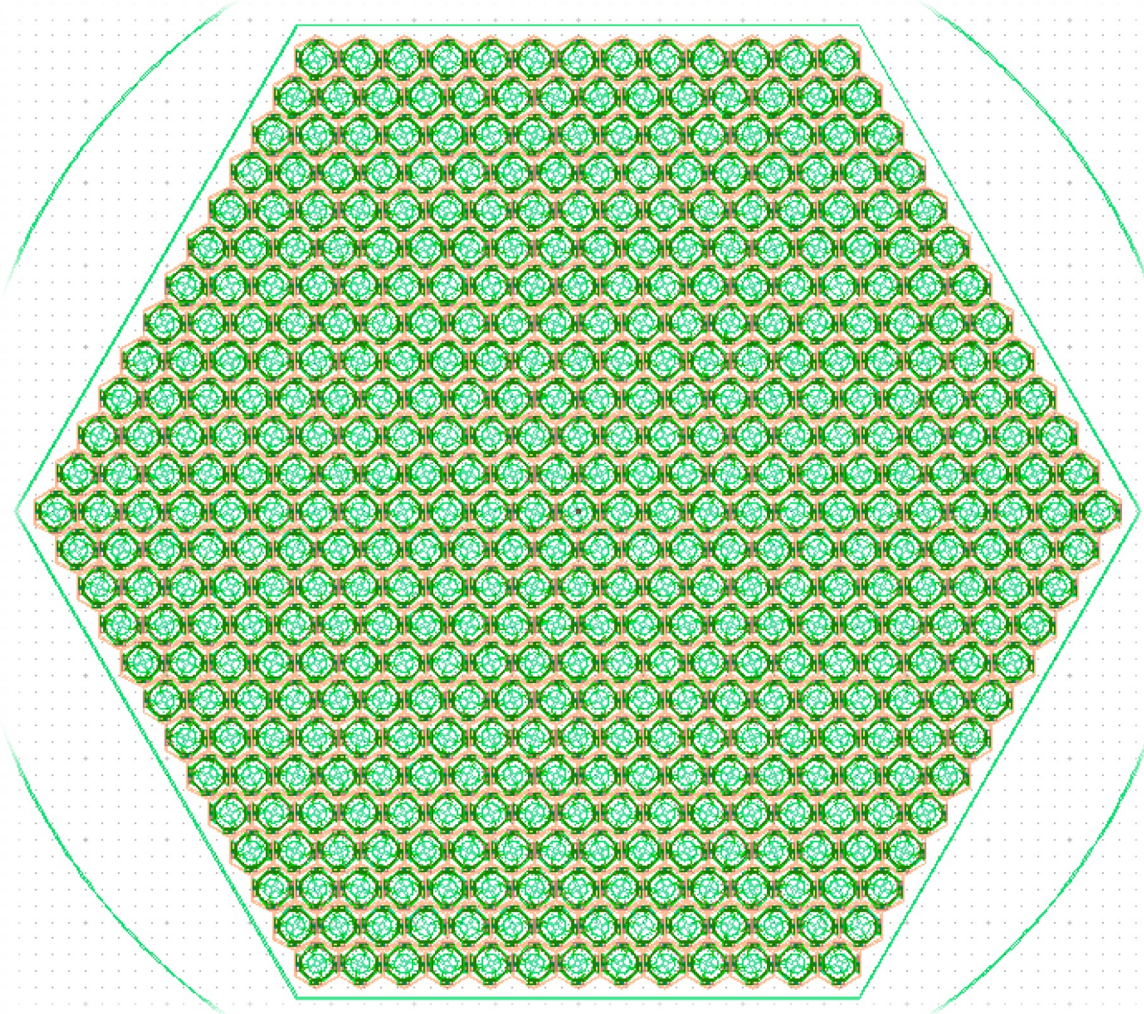
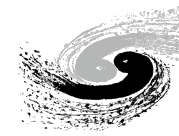
Picture credit: Victor Marin Felip, "The Search for Cosmic Inflation"

Application III: Cosmology

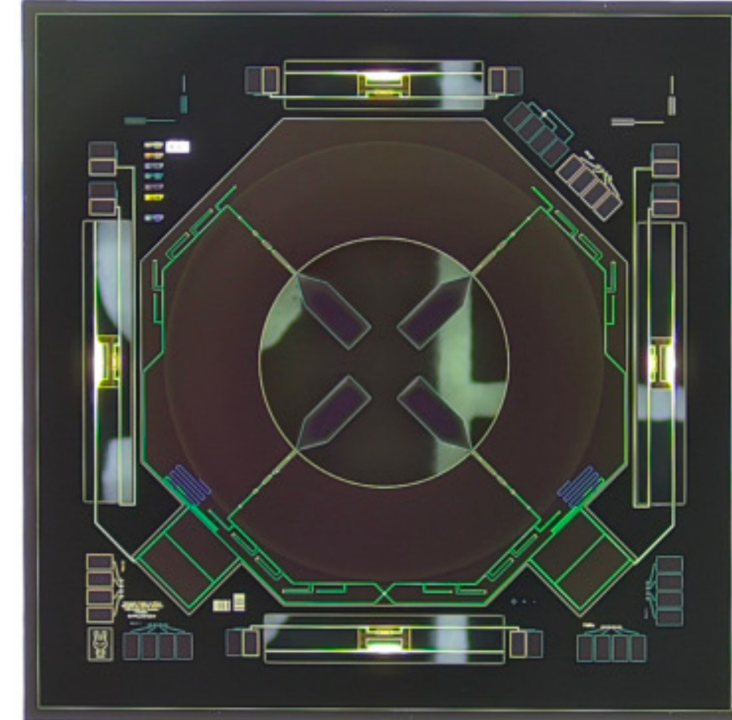


Picture credit: Herbert Huffner, "The Beginning of the World We Know"

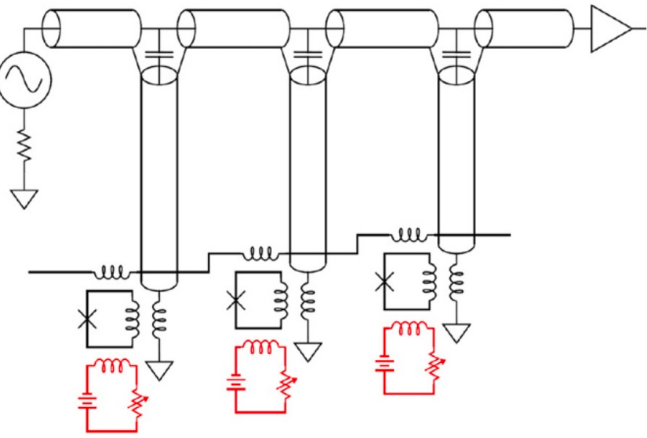
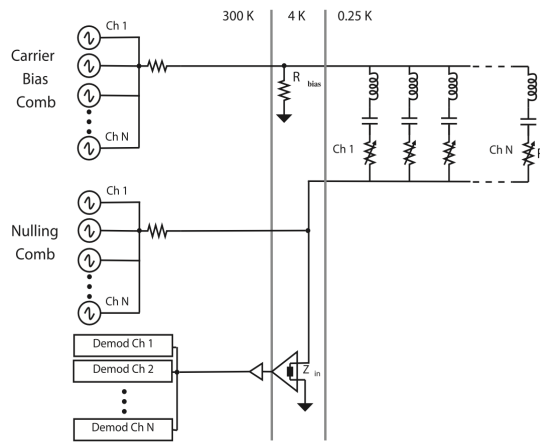
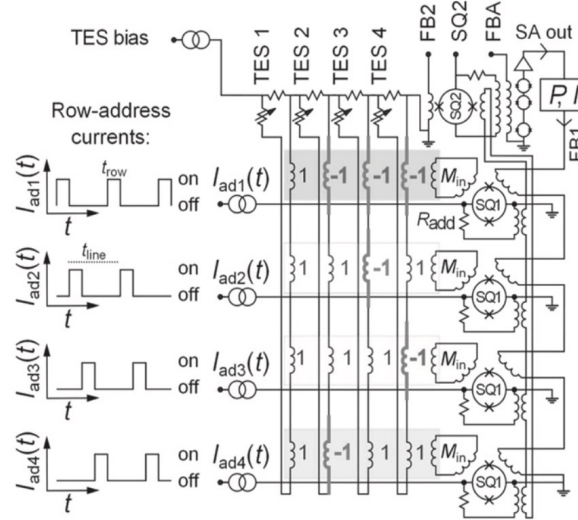
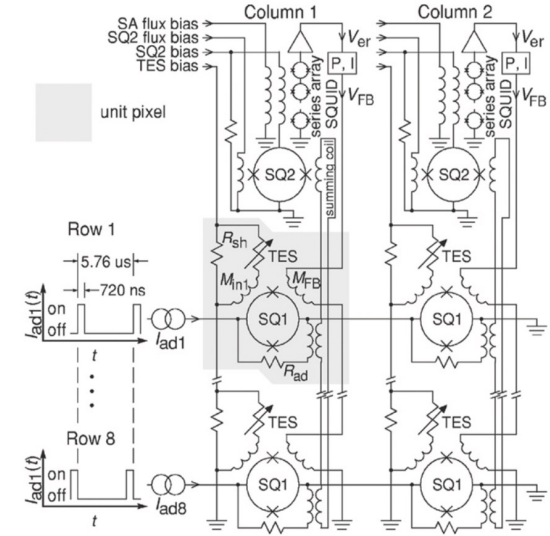
Application III: Cosmology



6-inch wafer
432 pixels per array
4 TESs per pixel

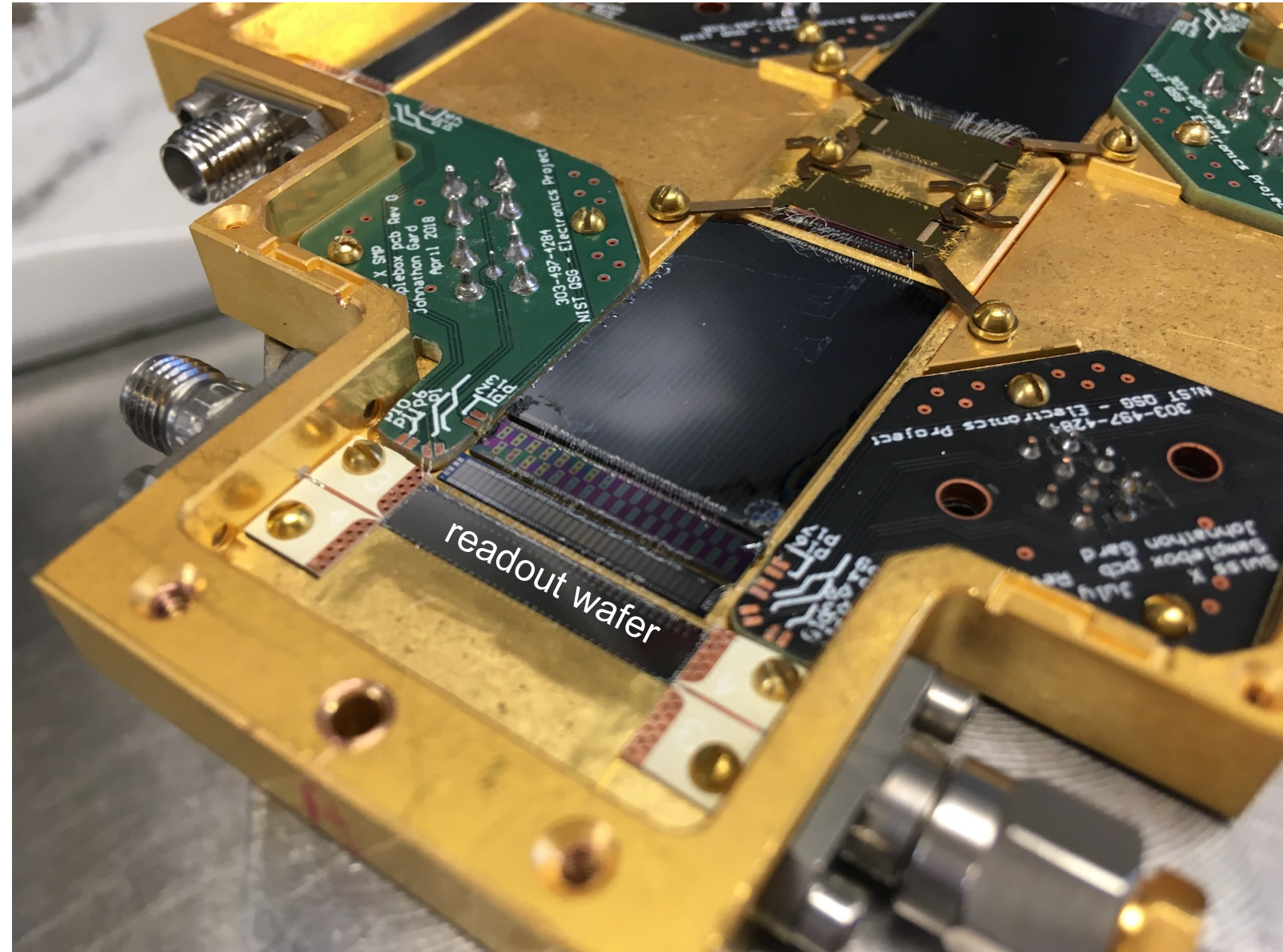
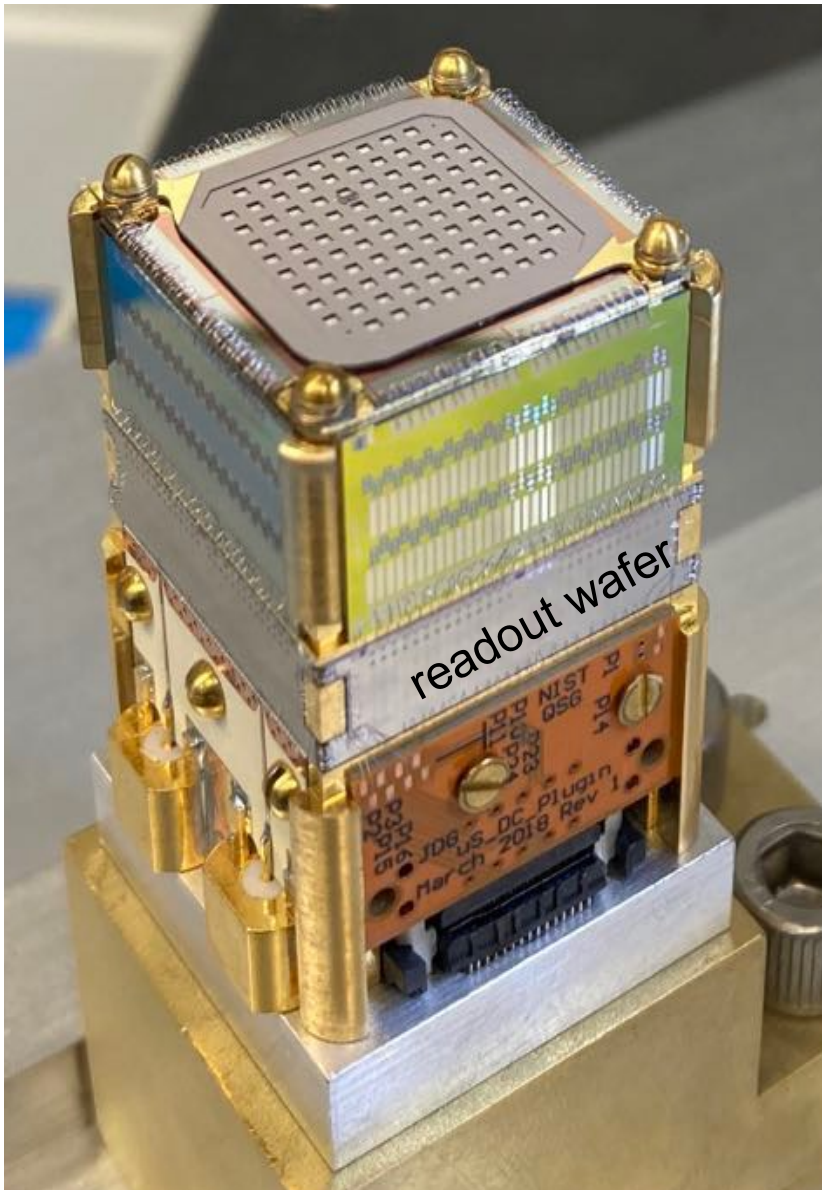
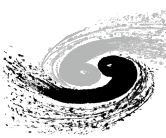


Low-Temperature Multiplex Readout



	time-division multiplexing	code-division multiplexing	frequency-division multiplexing	microwave-squid multiplexing
Machanism	pixels in the same column are read out in time series	signals from each pixel are encoded and read out	each pixel is biased in a unique LCR circuit, and detected in a unique frequency channel	TES signal coupled to rf-SQUID, then readout by microwave resonators
Advantage	well-developed technology	each pixel can be biased individually	each pixel can be biased individually	large readout bandwidth, only uses 3 pairs of cables for the whole detector module
Disadvantage	\sqrt{N} sampling noise	one bad pixel kills a whole column	complicated matching between TESs and the readout electronics	pixels are not individually biased, subject to nonuniformity across large arrays

Detector Assembly



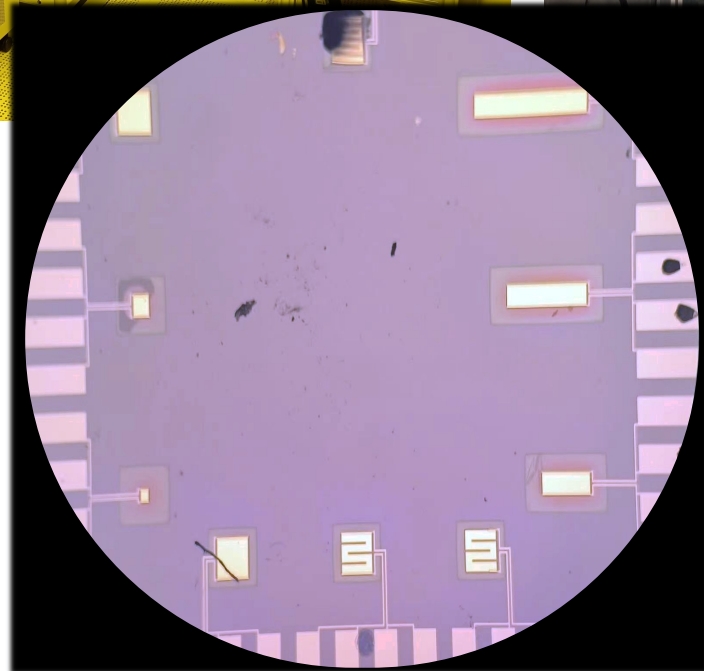
Research at IHEP: R&D



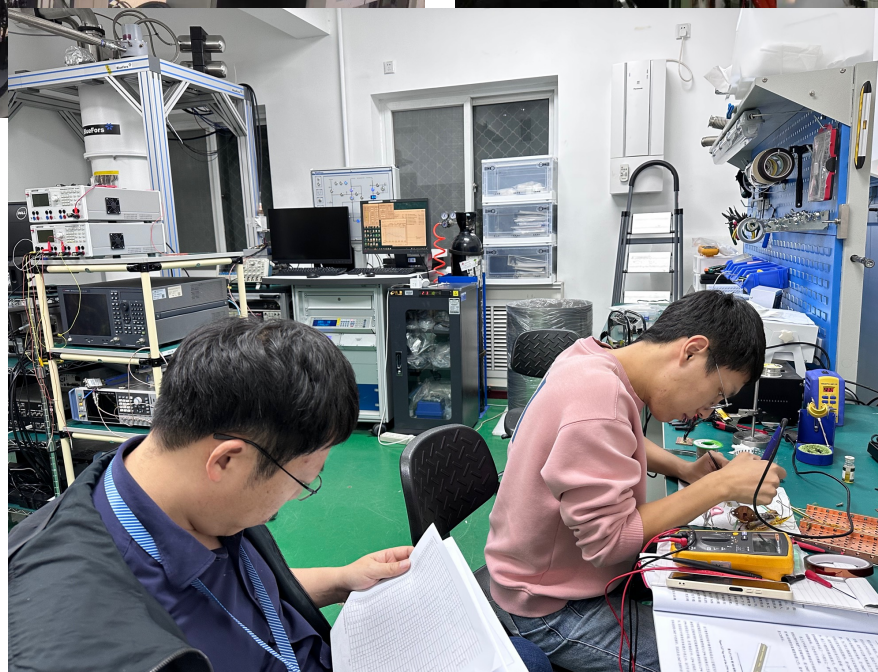
中國科學院高能物理研究所
Institute of High Energy Physics, Chinese Academy of Sciences

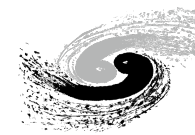


Fabrication



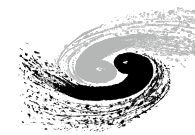
Characterization





What we do:

1. superconductor detector development (mainly TES, and for various applications)
 - overall design
 - device fabrication
 - detector characterization
2. low-temperature multiplexing readout electronics (SQUID)
3. room-temperature detector control & data taking electronics
4. data processing
 - photon signal analysis and optimization



What we do:

1. superconductor detector development (mainly TES, and for various applications)
 - overall design
 - device fabrication
 - detector characterization
2. low-temperature multiplexing readout electronics (SQUID)
3. room-temperature detector control & data taking electronics
4. data processing
 - photon signal analysis and optimization

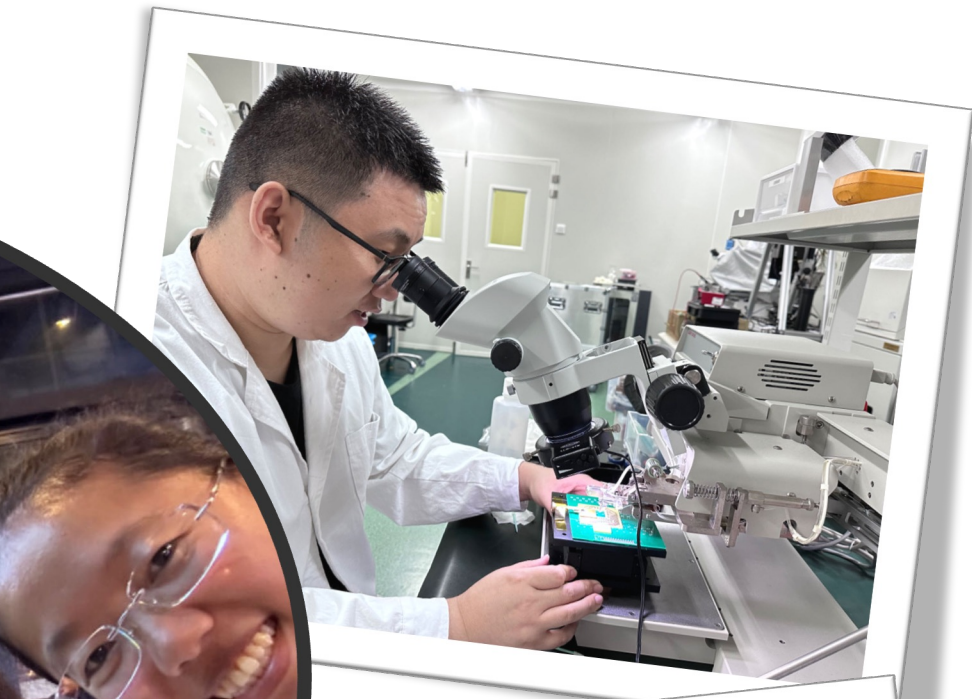
We are looking for postdocs and students!

Daikang Yan (闫代康): yandk@ihep.ac.cn, yandaikang@gmail.com

Research at IHEP: Life



中國科學院高能物理研究所
Institute of High Energy Physics, Chinese Academy of Sciences



Daikang Yan - IHEP

Research at IHEP: Life



中國科學院高能物理研究所
Institute of High Energy Physics, Chinese Academy of Sciences



Visit our superconducor device lab,
start your low-resistance journey!

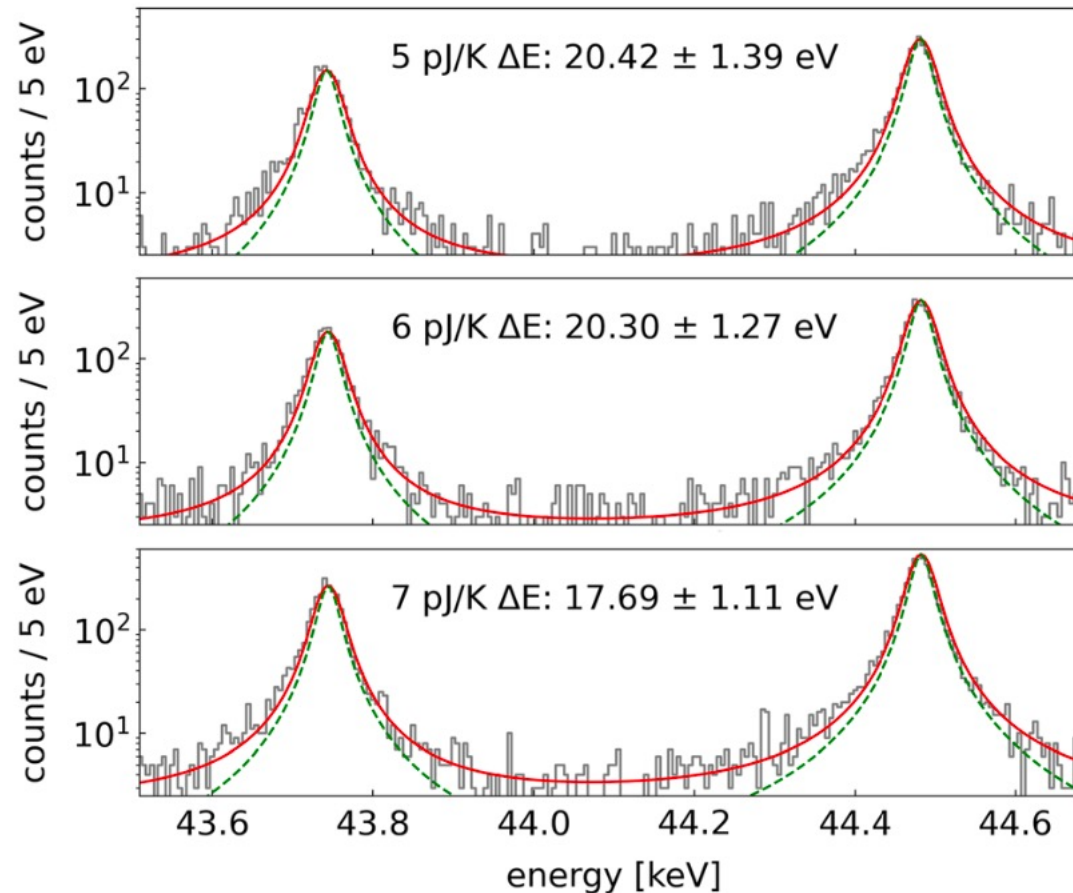
We are looking for postdocs and students!

Daikang Yan (闫代康): yandk@ihep.ac.cn, yandaikang@gmail.com

Daikang Yan - IHEP



Application II: QED



More results to come in 2024.....

Application II: QED

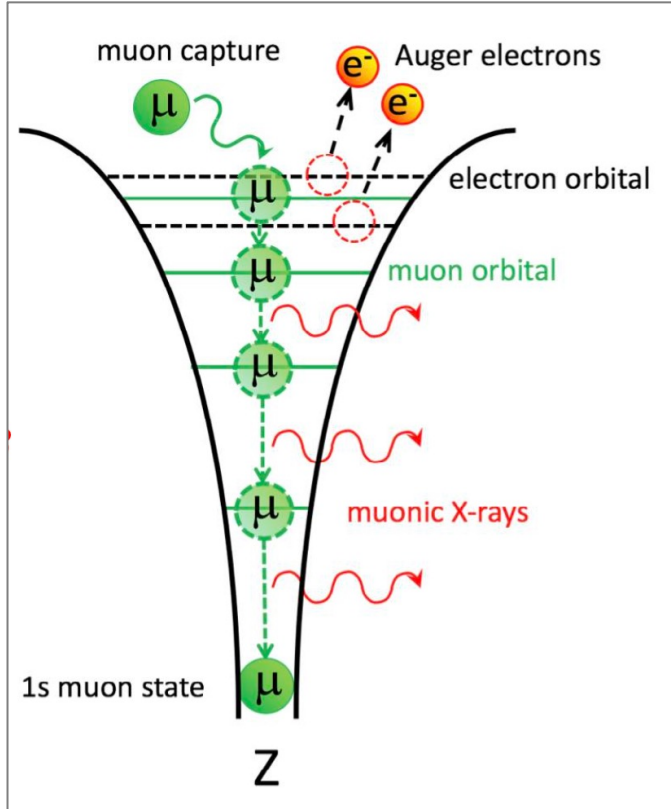
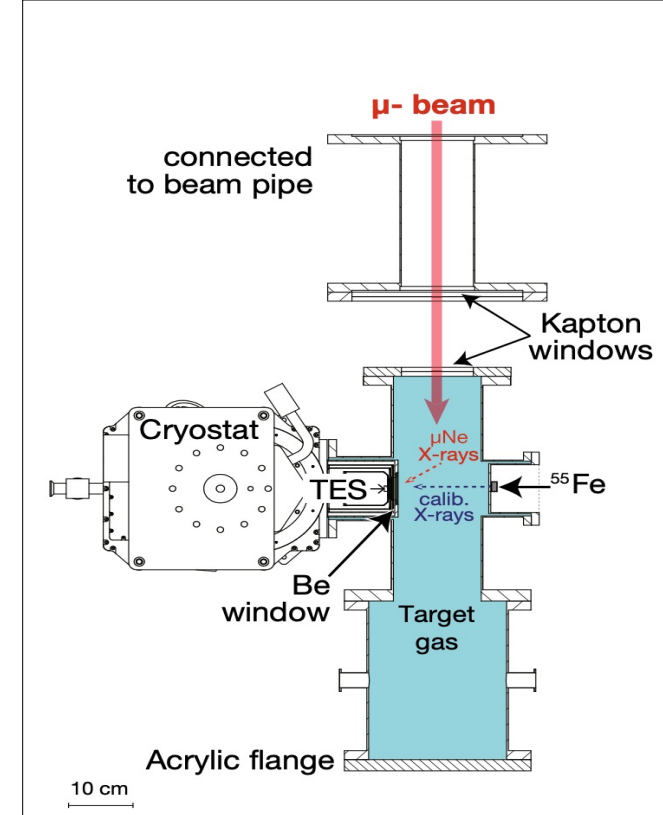


Figure credit: T. Okumura, RIKEN

Limitation/Requirement:

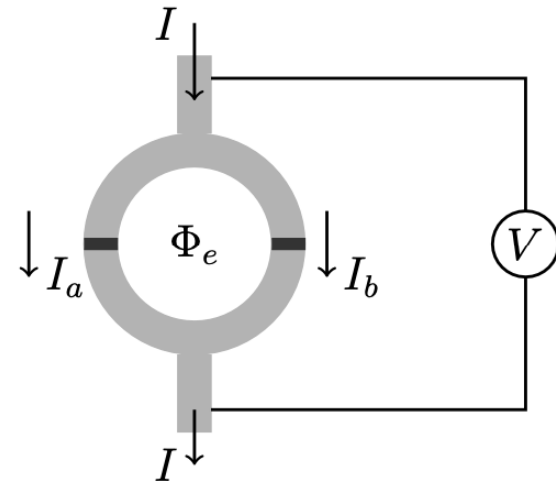
- 1) target atom low density
- 2) high energy resolution



S. Okada et al., Journal of Low Temperature Physics (2020)
200:445–451



DC-SQUID



RF-SQUID

